Gadolinium-Based Macrocyclic MRI Contrast Agents

Stephen Hopkins
Senior Honors Thesis
Dr. Erich Uffelman

Acknowledgments

I would first like to thank all former and current Uffelman group members that I have been given the opportunity to work with during these last four years. The projects contained in this thesis are the work of many students. Some of these students taught me an indescribable amount of chemistry. Some of these students I attempted to pass on my knowledge.

The first person I want to thank is Leonard Rorrer. Any lab knowledge or skill I have came directly from him. From talking to him or just watching him fiddle with a reaction, I learned to have confidence in my work and I learned the skills behind the confidence. He was one of those people that everyone around knew he would do something great.

I would also like to thank the students I had the chance to work with in my last summer of research at Washington and Lee. I can only hope that I did as good of a job as Leonard did in training them. I want to thank Ashley Shreves and Alison Cartwright for simplifying the early steps in the H_4 Hexadentate Tetraamide Macrocycle synthesis. Both of you were so much fun to work with for that last summer. Your energy and spunk brought new life to the lab. During those long hours of fall term research, I excitedly looked forward to the one day a week you two would be working. Also, I would like to thank Tom Stoklasek for all his time and effort helping me with "my" reactions. I wish him well in his future dealings.

The student I would most like to thank is Michele Connors. I worked with Michele for two of the three summers and most of the research during the years. While

we were on the same level in the lab, I always looked up to her for guidance in all of our other dealings. I will never have the words to properly thank her for all that she has done.

Many professors of the Washington and Lee faculty have helped me a tremendous amount. I would first like to thank my advisor, Dr. Erich Uffelman. No other person has ever taught me more about a subject than Dr. Uffelman has. It still baffles me how much I have learned about chemistry in four short years. I can only hope to have the ability to teach someone half of what Dr. Uffelman has taught me.

I would also like to thank Dr. Marcia France for all her teachings and guidance. She helped me more than many others during a very rough time. I want to thank Dr. Steven Desjardins for always showing me that I'm making it harder than it needs to be. I want to thank Dr. Matthew Tuchler for all his help in my last summer of research. He showed me that it truly is worth that last bit of effort to make something right. I would also like to thank Dr. J. Brown Goehring for all his insightful proofreading. Lastly, I want to thank Dr. Lisa Alty for just being fun. Even while learning a tremendous amount in her classes, I also truly enjoyed attending them.

For financial funding I would first like to thank Washington and Lee University's Robert E. Lee research grant. This grant has allowed me to work on these projects for almost three years now. I would also like to thank the Petroleum Research Fund, the Research Corporation, and the NSF-ILI.

To My Father,

I never could have made it this far without you

Table of Contents

Abstract

The early detection of diseased and cancerous cells leads to a dramatic increase in the survival rate of the patients. The limitations of magnetic resonance imaging (MRI) to differentiate many types of cancerous tissues from healthy tissue has led to a new pharmaceutical field. This new field aims to develop new metal complexes responsible for increasing the ability of MRI to detect the tumor. These paramagnetic metal-based complexes create a contrast between tumor tissue and healthy tissue. The first approved gadolinium-based macrocyclic contrast agent, $[Gd(DOTA)]^-$, created an effective contrast while remaining stable *in vivo*. Much research has been directed towards improvement of this complex through modification of the ligand.

In addition to research towards the betterment of the $[Gd(DOTA)]^-$ complex, many research groups have focused on the development of novel gadolinium complexes. Two such complexes, the $[Gd(Texaphyrin)]^{2+}$ complex and the [Gd(PCTA)] complex, have been shown to provide an increased contrast. These two complexes represent the most recent advances in contrast agent technology.

Research in the Uffelman group centers on the development of a novel MRI contrast agent by expanding the coordination chemistry of lanthanide ions to amido-N ligands. The group has successfully synthesized a H_4 pentadentate tetraamide macrocycle through a new, less dangerous intermediate. Significant steps have been taken towards the completion of an H_4 hexadentate tetraamide macrocycle. This larger ligand may have a greater chance of binding a lanthanide series ion.

List of abbreviations:

Cyclen	1,4,7,10-tetraazacyclododecane
BB-PCTA-[12]	12-(4-bromobenzyloxy)-3,6,9,15-tetraazabicyclo[9.3.1]pentadeca-1(15),11,13-triene-3,6,9-triacetic acid
DO3A	1,4,7-tris(carboxymethyl)-1,4,7,10-tetraazacyclododecane
DOTA	1,4,7,10-tetraazacyclododecane- N, N', N'', N'''-tetraacetic acid
DTPA	diethylenetriaminepentaacetic acid
EDTA	ethylenediaminetetraacetic acid
G3(N[CS]N-bz-{DO3A}$_{23}$	Generation three-1-(4-isothiocyanatobenzyl)-methylcarbamoyl-4,7,10-tri(acetic acid)tetraazacyclododecane
HP-DO3A	1,4,7-tris(carboxylmethyl)-10-(2-hydroxypropyl)-1,4,7,10-tetraazacyclododecane
NMRD	nuclear magnetic relaxation dispersion
PCTA-[12]	3,6,9,15-tetraazabicyclo[9.3.1]pentadeca-1(15),11,13-triene-3,6,9-triacetic acid
PCTA-[13]	3,6,10,16-tetraazabicyclo[10.3.1]hexadeca-1(16),12,14-triene-3,6-10-triacetic acid
(phen)HDO3A	1,4,7-tris(carboxymethyl)-10-phenanthroline-1,4,7,10-tetraazacyclododecane
PIP-bis(DO3A)	1,4-bis {[4,7,10-tris(carboxymethyl)-1,4,7,10-tetraazacyclododecan-1-yl]acetyl}piperazine
Texaphyrin	4,5-diethyl-10,23-dimethyl-9,24-bis(3-hydroxypropyl)-16,17-(3-hydroxpropyloxy)-13,20,25,26,27-pentaazapentacyclo [20.2.1.1^{3,6}.1^{8,11}.0^{14,19}]heptacosa-1,3,5,7,9,11 (27),12,14,16,18,20,22(25),23-tridecaene
Texaphyrin (Dimer)	Two Texaphyrin ligands bridged by gluconolated 1,4,8,11-tetraazacyclotetradecane

Chapter I

Introduction and Theory

The early detection of diseased and cancerous cells leads to a dramatic increase in the survival rate of the patient. The ability to effectively image soft tissue samples has recently caused magnetic resonance imaging (MRI) to become the most widely used method of detection. While excellent at imaging this soft tissue, MRI fails to distinguish many types of cancer cells from healthy cells. Imaging tumors found in the human breast proved difficult for this reason.[1] This problem spawned a new pharmaceutical field aimed at the development of compounds responsible for increasing the ability of MRI to detect the tumor.[2-5] These paramagnetic metal-based complexes create a contrast between the tumor tissue and the healthy tissue by exploiting the different environments of the two types of cells. This new ability to create a contrast has led to many other applications of MRI. One such application uses contrast enhanced MRI to image blood flow in the vascular system.[6] The design requirements of these complexes center on the ability of the complex to effectively create a contrast, thermodynamic and kinetic stability, and the overall charge of the complex. Before any discussion of specific metal complexes can be made, an appreciable level of knowledge of how MRI works along with the theory behind rational ligand design must be understood.

Magnetic Resonance Imaging is a noninvasive method of imaging human tissues. Unlike high-energy x-ray methods, such as computerized axial tomography (CT), MRI uses low energy radiofrequency waves to image the tissue. This dramatic decrease in energy of the imaging photon causes much less tissue damage. Lauffer[2] gives an informative description of the main principles behind MRI techniques. Also, less detailed but more up-to-date information can easily be found on the internet.[7,8] First, the patient is exposed to a linear magnetic field gradient. In the magnetic field, the ^{1}H nuclei

of water have a nuclear spin of ½. When exposed to the magnetic field, the nuclei can occupy one of two possible spin states. A little more than half of the nuclei move to the lower energy spin state and align with the magnetic field (defined as the z-axis). The remaining nuclei align opposite to the magnetic field and enter a higher-energy state. This alignment creates a net macroscopic magnetization vector along the z-axis. As the nuclei spin, they also precess or wobble at a certain frequency called the Larmor frequency.[7] Radiofrequency pulses (tuned to the Larmor frequency) then tip the net macroscopic magnetization vector off the z-axis and into the x-y plane. The time it takes the vector to return to the equilibrium state can be measured. This relaxation time is described using the exponential time constant T_1, the longitudinal relaxation constant or spin-lattice constant. The T_2, transverse relaxation constant or spin-spin constant, measures the time for the magnetic vector perpendicular to the z-axis to return to its equilibrium value of zero. Most research aims at exploiting T_1 because the length of T_2 is very short and is not easily changed under safe conditions. The combined data of the two relaxation constants gives the water signal intensity.[4] The MRI spectrometer measures the water signal intensity along a thin three-dimensional "slice" of the target area. Each "slice" contains multiple volume elements called voxels that have a volume of about 3 mm^3.[8] The water signal intensity measured for each voxel can be used to spatially localize the water molecules. The spatially localized intensity data is then transformed into a three-dimensional view of the target area.

For an effective three-dimensional view, the contrast agent must preferentially reduce the proton relaxation time of the tumor tissue over the healthy tissue. The most direct way of accomplishing this is to create a contrast agent concentration gradient by

localizing the contrast agent into the tumor tissue. Creating this concentration gradient proves rather difficult and is an active area of research.[9] Because a tumor-targeting contrast agent has not yet successfully been developed, the contrast must be created by exploiting the differing environments of the water in the tumor tissue versus the water in the healthy tissue. A contrast agent can be tailored to preferentially enhance the relaxation of tumor tissue environment while not maintaining a preferential concentration gradient.

The ability to enhance the relaxation of the water molecule in the tumor tissue comes from the paramagnetic metal center of the contrast agent. To display paramagnetism, a metal simply must contain unpaired electrons. Exposure to the paramagnetic metal substantially decreases the relaxation time of the water proton.[4] This ability to decrease the relaxation rate of water is defined as relaxivity. More precisely, relaxivity, R_i, is the slope of the relaxation rate of the solvent (in this case water) versus the concentration of paramagnetic species ($mM^{-1}\ s^{-1}$).[2]

Early research centered around transition metals and rare earths (Mn, Fe, ^{51}Cr, Gd, Yd, Dy).[3] It was first thought that using metals that appeared in trace amounts in the body would be less toxic. For this reason the initial research explored the use of Mn(II) and Fe(III). Trace metals, however, can become toxic if concentrations become too high. Because of its great amount of paramagnetism, gadolinium(III) proved to be much more promising. In the +3 state, gadolinium is f^7 with seven unpaired electrons. This makes gadolinium the single most paramagnetic metal ion known.

While the paramagnetic nature of gadolinium(III) is ideal for creating a contrast agent, the metal is very toxic and human tolerance levels are low.[2,4] The LD_{50} (lethal

dose of half of the participants) of $GdCl_3$ in rats has been shown to be 0.5 mmol/kg.[5] Gadolinium(III) has been shown to bind to serum proteins and may bind ligands like citrate. Exposed Gd(III) probably hydrolyzes to a hydroxide that is then taken up into the reticuloendothelial system.[3] This causes accumulation in the liver, spleen and bone marrow.[3,5]

Chelation of the Gd(III) ion to an organic ligand masks the high toxicity of the metal ion by nearly 100 fold.[3,4] The reduction of toxicity, however, hinders the ability of the contrast agent to provide a contrast. Both open chain ligands as well as macrocyclic ligands effectively chelate Gd(III). Attempts to use the open chain EDTA (Figure 1) seemed promising because of high relaxation effects.[2] Research ceased due to the high levels of toxicity shown by the $[Gd(EDTA)]^-$ complex (levels ranged close to that of $GdCl_3$). EDTA does not bind the Gd tightly and therefore releases the metal *in vivo* rather easily. Gadolinium(III) complexes of the open chain ligand DTPA (Figure 2) show much lower toxicity while still retaining effective relaxation effects. This ligand is one of two open chain ligands approved for clinical application. While $[Gd(DTPA)]^{2-}$ is thermodynamically stable, recent evidence suggests the kinetic stability is more important.[5] The ligand appears to preferentially bind Zn(II) from the body and release the Gd(III). The effectiveness of the $[Gd(DTPA)]^{2-}$ complex as a contrast agent is greatly reduced since the ligand is not kinetically inert.

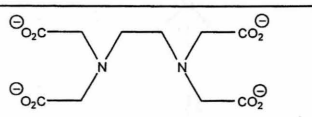

Figure 1: EDTA

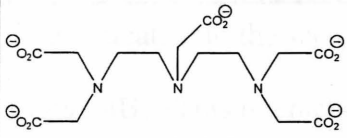

Figure 2: DTPA

Macrocyclic ligands have been shown to increase selectivity for Gd(III) over Zn(II). Gadolinium(III) complexes of the macrocyclic ligand DOTA (Figure 3) gave

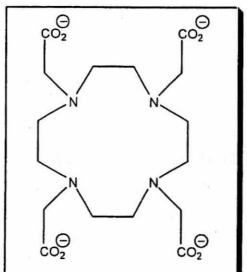

Figure 3: DOTA

early success in T_1 relaxation effects. The $[Gd(DOTA)]^-$ complex has also been shown to have relatively low toxicity.[1] After injection of the clinical dose (0.1 mmol/kg), the chelate is excreted from the body before an appreciable equilibrium between trace body metals can be met.[3]

The chelated Gd complex affects relaxation times through two distinct mechanisms: inner sphere and outer sphere.[2-4] When a water molecule enters into the coordination sphere of the Gd-chelate and directly binds to the metal (Figure 4A), the inner sphere mechanism dominates. This type of interaction is the most direct way of communicating between the paramagnetic center and the bulk water and therefore yields the highest amount of relaxivity. The metal center can also communicate into the second coordinate sphere through hydrogen bonding of its ligands (Figure 4B). This interaction combined with bulk diffusion past the paramagnetic chelate (Figure 4C) gives the outer sphere mechanism.[2] The measurable relaxivity can easily be found by adding together the inner sphere contribution and the outer sphere contribution; equation (1).

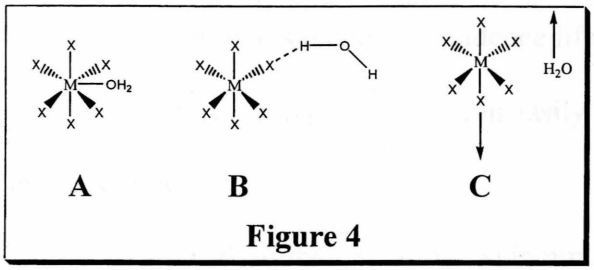

Figure 4

$$R_{1p}^{meas} = R_{1p}^{is} + R_{1p}^{os} \quad (1)$$

The R_{1p}^{meas} is the measured relaxivity, the R_{1p}^{is} is the contribution from the inner sphere and the R_{1p}^{os} is the contribution from the outer sphere.

The exact description of the inner sphere contribution is difficult to represent. The Solomon-Bloembergen-Morgan theory must be used to fully describe the contribution. Equations (2)-(5) describe this theory.[1,4,5]

$$R_{1p}^{is} = (cq/55.6)(1/(T_{1M} + \tau_M)) \quad (2)$$

$$1/T_{1M} = (K/r^6)f(\tau_c,\omega_I,\omega_S) \quad (3)$$

$$1/\tau_c = 1/\tau_R + 1/\tau_S + 1/\tau_M \quad (4)$$

$$1/\tau_S = (1/5\tau_{SO})((1/(1+\omega_S^2\tau_v^2))+(4(1+4\omega_S\tau_v^2))) \quad (5)$$

In equation (2), c is the molar concentration of the paramagnetic complex, q is the number of bound water molecules, T_{1M} is the longitudinal proton relaxation time of the bound water and τ_M is the mean residence life of the bound water. The inverse relationship between R_{1p}^{is} and T_{1M} can easily be stated as a reduction in T_{1M} leads to an increase in R_{1p}^{is}.

Lauffer[2] describes equation (3) in much greater detail than the equation shown. The physical description behind the constant K is not needed for this discussion and is therefore not shown. Also, $1/T_{1M}$ is only shown as a function of τ_c (the correlation time for the modulation of the dipolar interaction), ω_I (the Larmor frequency for the proton), and ω_S (the Larmor frequency for the electron). The actual function is not needed and is therefore also not given. Notice also that r (the distance between the metal ion and the water molecule) is raised to the sixth power. This shows that increasing the distance between the metal ion and the water molecule leads to a rapid increase of $1/T_{1M}$. This increase of $1/T_{1M}$ reduces the overall relaxivity.

Equation (4) delves deeper into the theory and shows many interesting ways to manipulate the overall relaxivity. The τ_c constant is inversely dependent on τ_R (the

rotational tumbling time of metal complex with water), τ_S (the longitudinal electron spin relaxation time), and τ_M (the mean residence life; the same as in equation (2)). A variation of these three constants can lead to profound changes in relaxivity. This idea will be discussed in subsequent chapters.

Equation (5) shows how τ_S is dependent on τ_{SO} (value of the electronic relaxation time at zero field), τ_v (correlation time characterizing the time dependence of the interaction), and ω_S (the Larmor frequency for the electron; same as for equation (3)). Many Gd(III) complexes used as contrast agents have a high level of symmetry. These compounds typically undergo zero-field splitting (ZFS) of the electronic spin levels. The ZFS in turn causes electronic relaxation that must be accounted for by theories. Collisions from solvated water molecules further complicate the situation as they perturb and distort this symmetry of the complex thereby causing transient ZFS.[2] The transient ZFS must also be energetically accounted for by theories. Equation (5) attempts to account for this transient relaxivity. To describe the transient ZFS of complexes with lower symmetry, much more complicated theories must be used. These theories assume much less about the nature of rotational modulation of the ZFS tensor.[2]

Equations (2)-(5) describe physical attributes of the Gd-complex. These equations provide researchers with a "road map" on how to manipulate future compounds to increase relaxivity. The rotational motion (τ_R) is the easiest to manipulate and has therefore been a topic of much research.[5] Simply changing the molecular weight of the complex has a profound effect that will be explored in Chapter II.

The outer sphere mechanism also contributes to the overall relaxivity of the Gd-complex.[2-4] Since its effects are not as great (and are also harder to control), researchers

have neglected its importance. Freed's equation is commonly used to describe this mechanism; equation (6).

$$R_{1p}^{os} = (32\pi/405)\gamma_H^2 g^2 \mu_B^2 S(S+1)* \\ (N_A/1000)*(C/aD)f(\tau_S, \tau_D, \omega_S, \omega_I) \qquad (6)$$

In equation (6) the γ_H represents the proton magnetogyric rate, the g is the Lande factor, μ_B is the Bohr magneton, S is the total electron spin of the Gd(III) ion ($^7/_2$), N_A is Avagadro's number, C is a constant, a is the distance between the closest approach of the water molecule to the Gd(III) center, D is the relative translational diffusion of solute and solvent, and $\tau_D = a^2/D$. This complicated equation attempts to relate the effects of electronic relaxation to the effects of translational diffusion.[2]

All of these equations can be used to gain structural information about the binding of water molecules.[2,4] Through the use of magnetic field dependent studies a nuclear magnetic relaxation dispersion (NMRD) plot can be generated. This plot shows how the relaxivity is dependent on the magnetic field. High relaxivity in the high magnetic field region (10-15 MHz) indicates a large dependence on τ_R, the rotational motion of the complex. High relaxivity in the low magnetic field region reveals increasing involvement of τ_S, the longitudinal electron spin relaxation time.

Unlike the inner sphere/outer sphere theory, the overall charge of the complex does not affect the relaxivity. Instead, the overall charge affects the use of the complex. Complexes with a negative charge quickly excrete through the kidneys. Negatively charged species are most appropriate for imaging tumors of the kidneys or blood flow through the kidneys. Most positively charged species build up in the heart area. These types of contrast agents have potential application in detecting blood clots near the heart.

Also, to cross the blood-brain barrier, a neutral complex is needed.[5] Charged species may cause unneeded pain to the patient upon injection.

Manipulation of the Solomon-Bloembergen-Morgan equations allows for many different design motifs for potential contrast agents. Due to the high toxicity of free Gd(III), the first clinically used macrocyclic contrast agent used ([Gd(DOTA)]$^-$) sacrificed much relaxivity in the name of thermodynamic and kinetic stability.[10] Subsequent research has attempted to use Solomon-Bloembergen-Morgan theory to rationally design new contrast agents.[11] The next chapter will discuss the DOTA ligand in detail. It will also show current research into modifications of the ligand. Derivatives of DOTA have been shown to greatly increase relaxivity while maintaining a high level of stability. The third chapter will focus on new potential contrast agents unrelated to the DOTA ligand. These ligands explore new theories and ideas in attempts to achieve the same goals.

References

[1] Degani, H.; Gusis, A.; Weinstein, D.; Fields, S.; Strand, S. "Mapping pathophysilogical features of breast tumors by MRI at high spatial resolution." *Nat. Med.* **1997**, *3*, 780-782.

[2] Lauffer, R. B. "Paramagnetic Metal Complexes as Water Proton Relaxation Agents for NMR Imaging: Theory and Design." *Chem. Rev.* **1987**, *87*, 901-927.

[3] Thunus, L.; Lejeune, R. "Overview of Transition Metal and Lanthanide Complexes as Diagnostic Tools." *Coord. Chem. Rev.* **1999**, *184*, 125-155.

[4] Parker, D.; Williams, J. A. G. "Getting Excited About Lanthanide Complexation Chemistry." *J. Chem. Soc., Dalton Trans.* **1996**, 3613-3628.

[5] Reichert, D. E.; Lewis, J. S.; Anderson, CJ. "Metal Complexes as Diagnostic Tools." *Coord. Chem. Rev.* **1999**, *184*, 3-66.

[6] Bogdanov, A. A.; Weissleder, R.; Brady, T. J. "Long-circulating Blood Pool Imaging Agents." *Adv. Drug Delivery Rev.* **1995**, *16*, 335-348.

[7] MRI Tutor. http://128.227.164.224/mritutor/index.html (accessed April 2000)

[8] The Basics of MRI. http://www.cis.rit.edu/people/faculty/hornak/ (accessed April 2000)

[9] Lemieux, G. A.; Yarema, K. J.; Jacobs, C. L.; Bertozzi, C. R. "Exploiting Differences in Sialoside Expression for Selective Targeting of MRI Contrast Reagents." *J. Am. Chem. Soc.* **1999**, *121*, 4278-4279.

[10] Desreux, J. F. "Nuclear Magnetic Resonance Spectroscopy of Lanthanide Complexes with Tetraacetic Tetraaza Macrocycle. Unusual Conformation Properties." *Inorg. Chem.* **1980**, *19*, 1319-1324.

[11] Comblin, V.; Gilsoul, D.; Hermann, M.; Humblet, V.; Jacques, V.; Mesbahi, M.; Sauvage, C.; Desreux, J. F. "Designing new MRI Contrast Agents: A Coordination Chemistry Challenge." *Coord. Chem. Rev.* **1999**, *185-186*, 451-470.

Chapter II

The [Gd(DOTA)]$^-$ Contrast Agent

While much research has gone into the development of new contrast agents, $[Gd(DOTA)]^-$ remains the only clinically approved macrocyclic complex in the United States. In 1986, the European community, which has traditionally shown relaxed regulation in this field, became the first region to approve $[Gd(DOTA)]^-$ as a contrast agent.[1] Despite both European and American approval, the high cost of production prevented the use of $[Gd(DOTA)]^-$ as a contrast agent. A new synthetic route[2] has recently made the cost of production practical. This synthetic route will be discussed as will be the binding of the Gd(III) ion. The $[Gd(DOTA)]^-$ complex displays interesting coordination chemistry that directly leads to kinetic stability. The ability to remain kinetically inert safely allows $[Gd(DOTA)]^-$ to create an *in vivo* contrast. This high degree of stability has significantly reduced the relaxivity of the complex. Recently, researchers have begun to modify the DOTA ligand to increase the relaxivity. These new ligands derived from DOTA must remain kinetically stable to be effective contrast agents. In addition to simple adjustments of the DOTA ligand, researchers have also set out to create macromolecular compounds that incorporate multiple $[Gd(DOTA)]^-$ complexes into a single molecule. A quick glimpse into this developing field will show how macromolecular chemistry can be used to raise relaxivity.

Synthesis of the DOTA ligand

The high cost of producing the synthetic intermediate cyclen (Figure 1A) greatly impeded the use of $[Gd(DOTA)]^-$ as a contrast agent.[2] It was not until 1996 that a cheap synthetic route came available.[3,4] This new route (Figure 1) lowered the cost of production on industrial scale to $1000/kg. After completion of the cyclen intermediate, it is trivial to add the acetate pendant arms of the DOTA ligand. The coordination

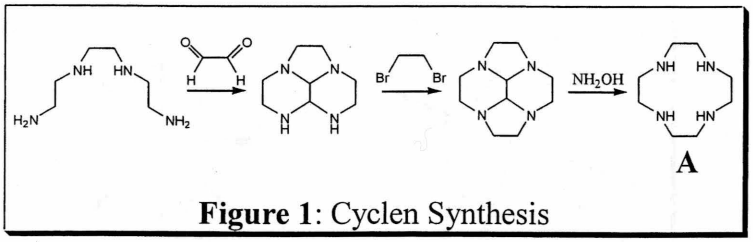

Figure 1: Cyclen Synthesis

environment of the DOTA ligand is vital in providing the interesting chemistry of the $[Gd(DOTA)]^-$ complex.

Coordination Chemistry of the DOTA Ligand

The interesting coordination chemistry of the DOTA (Figure 3, chapter I) ligand provides the complex stability needed for a MRI contrast agent. The amine nitrogens of the cyclen backbone possess the needed donor ability to bind a lanthanide series ion.[5] Lanthanide series ions behave much like Ca(II) ions and form electrostatic non-directional bonds. The lone pair of the amine nitrogen points inward towards the hard, polarizing ion.[6] This allows the amine nitrogen to form a tighter bond than an ether oxygen. The four acetate pendant arms, each carrying a single negative charge, offset the +3 charge of the metal ion. This combination of directional amine bonds with acetate bonds provides the stability needed for an affective contrast agent.

These eight ligating atoms of DOTA form a rare lanthanide complex with axial symmetry, shown by solid state NMR.[7] The cavity created by the cyclen backbone is too small to fit the Gd(III), so the metal ion must rest on top of the ring. The four pendant arms wrap around the metal ion forming a macrocyclic cage in an antiprismatic arrangement. This tight cage allows one water molecule to bind into the inner coordination sphere of Gd(III).[5]

The symmetric complex allows the 12 membered cyclen backbone to sit in its most stable conformation with the four CH_2 groups fully staggered.[2] Originally it was thought that this conformation was stable on an NMR time scale[7], but recent variable

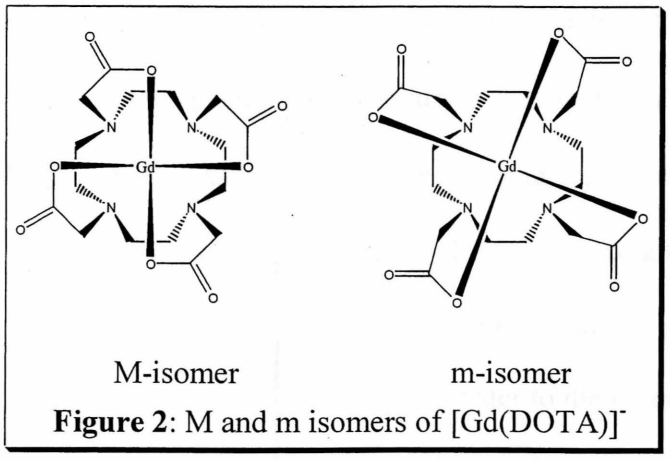

Figure 2: M and m isomers of [Gd(DOTA)]$^-$

temperature (VT) NMR studies[8] have revealed the presence of a diastereomeric pair (Figure 2).[9] The nomenclature of M (major isomer) and m (minor isomer) comes from studies performed on [Yb(DOTA)]$^-$ complexes.[10] In the study, the M-isomer was found in greater concentrations. Also, the M-isomer appears in the antiprismatic solid state structure of most lanthanide series DOTA complexes (Eu, Gd, Dy, Ho, Lu, and Y).[9] The m-isomer is seen in the twisted antiprismatic solid state structure of only a few lanthanide series DOTA complexes (La and Ce). Recent studies[10] indicate that actually the complex exists in two enantiomeric pairs of diastereomers

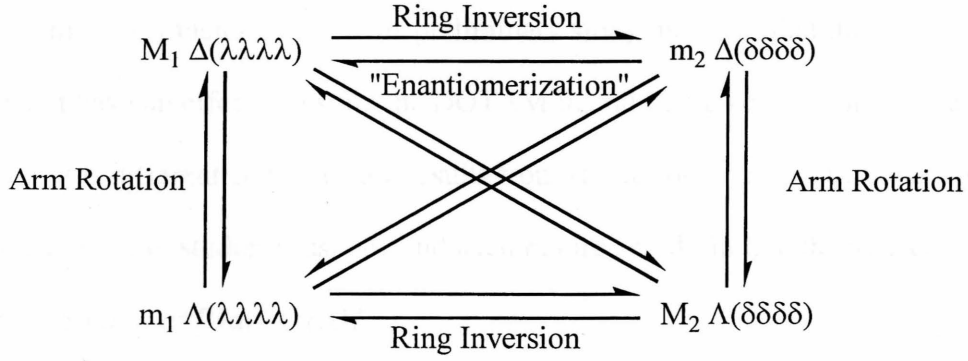

Figure 3: The Isomerization Process

(Figure 3).[9] The presence of two helices brings about these four stereoisomers. One helix derives from position of the pendant acetate arms and the other from the conformation of the cyclen backbone. Diastereomeric conversion due to a change in the acetate pendant arms is described by the Δ and Λ. Ring inversion of the cyclen backbone

also causes a diastereomeric conversion, denoted by δδδδ and λλλλ. Comparatively, rotation of the pendant arms occurs at a much faster rate than ring inversion.[10] Both a Δ-Λ and a δδδδ-λλλλ conversion must occur for enantiomerization, denoted by and subscripts 1 and 2.[9] It is not known whether this occurs successively or concurrently. Originally, it was thought that the binding of water to the inner coordination sphere of the metal ion had an effect on the isomeric conversions. This theory could never be validated because no bound water peak could be observed by NMR due to the quick exchange of water into the coordination sphere of $[Gd(DOTA)]^-$ ($k_{ex} = 4.1x10^6\ s^{-1}$ at 298 K).[9] A recent study[9] on the related ligand, DOTAM (Figure 4), gave the first bound water NMR signal. The replacement of carboxylate groups with amide groups slows down the water exchange by approximately a factor of 15. This preliminary study indicates that the binding of water does not have an effect. Despite the DOTAM ligand being very similar to the DOTA ligand, it is different and therefore results from studies on it cannot be universally applied. Further studies must be conducted before any definitive theories can be stated.

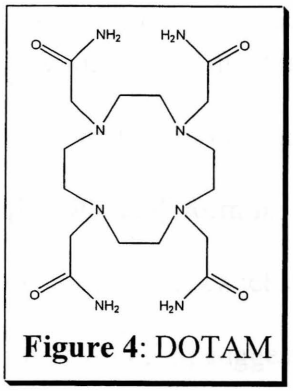

Figure 4: DOTAM

Kinetic Studies of [Gd(DOTA)]⁻

The tight macrocyclic cage formed around the Gd(III) provides the kinetic inertness and thermodynamic stability needed for the complex to perform as a contrast agent.[2,11] While lanthanide ions associate and dissociate quickly from open chain ligands, dissociation from macrocyclic ligands proceeds at a slower rate. An in-depth study of the kinetics of association and disassociation performed by Wang et al.[11] provided a considerable amount of data. The slow complex formation proceeds through a

two step process: the quick formation of a stable intermediate followed by the rate-determining step of completing the caged metal. This is illustrated by equations (1)-(3).

$$M + L \rightleftharpoons (ML)^* \quad \text{equilibrium constant } K^* \qquad (1)$$

$$(ML)^* \longrightarrow ML \quad \text{kinetic constant } k^* \qquad (2)$$

$$M + L \longrightarrow ML \quad \text{Kinetic constant } k_f \qquad (3)$$

The kinetics of most lanthanide series reactions cannot distinguish between the combination of (1) and (2) and the direct complexation displayed in (3). The $[M(DOTA)]^-$ forming reaction, however, proceeds slowly enough that the (ML)* can be observed. The exact structure of (ML)* is not yet known. Kinetic experiments (in a pH range of 4.5-6) suggest that the intermediate is the doubly deprotonated form of the ligand, H_2L^{2-}. Equation (4) denotes the observed kinetics.

$$k_{obs} = (k_f[M])/(1+K^*[M]) \qquad \text{where } k_f = k^*K^* \qquad (4)$$

This equation can be rearranged into equation (5).

$$1/k_{obs} = 1/(k_f[M]) + K^*/k_f \qquad (5)$$

This indicates a second order rate constant. As predicted, a plot of $1/k_{obs}$ versus $1/[M]$ yields a straight line.[11] Three species can contribute to the kinetics of complexation: H_3L^- (the singly deprotonated form), H_2L^{2-} (the doubly deprotonated form) and HL^{3-} (The triply deprotonated form). This yields the rate law shown in equation (6).

$$d[ML]/dt = k_f[M][L]_{tot} =$$

$$[M](k_{f,H3L}[H_3L^-] + k_{f,H2L}[H_2L^{2-}] + k_{f,HL}[HL^{3-}]) \qquad (6)$$

Rearrangement yields

$$k_f = k_{f,H3L}\alpha_{H3L} + k_{f,H2L}\alpha_{H2L} + k_{f,HL}\alpha_{HL} \qquad (7)$$

$$\alpha_{HnL} = \beta_n[H^+]^2/(1+\beta_1[H^+] + \beta_2[H^+]^2 + \ldots + \beta_n[H^+]^n) \qquad (8)$$

$$\beta_n = ([H_nL^{(4-n)-}])/([H^+]^n[L^{4-}]) \qquad (9)$$

with β_n as the overall formation constant. If one of the three contributing species is particularly more reactive than the other two, then equation (7) reduces to equation (10).

$$\log k_f = \log k_{f,HnL} + \log \alpha_{HnL} \qquad (10)$$

For this to hold true, a plot of log k_f versus log α_{HnL} will give a straight line of slope 1.0. All calculations failed to produce a slope of 1.0, therefore no single species solely accounts for the intermediate. With a slope of 0.71, the H_2L^{2-} species did attain the closest result. These data coupled with experimental results further suggest H_2L^{2-} as the primary intermediate species. When attempting to calculate the rate constants of each species, inclusion of the L^{4-} species and the H_3L^- species into the calculations continually led to negative results. If only the HL^{3-} species and the H_2L^{2-} species are taken into account, the calculations agreed greatly with the previously mentioned experimental results. These rate constants are

$$k_{f,HL} = (1.0 \pm 0.8) \times 10^6\ M^{-1}\ s^{-1}$$

$$k_{f,H2L} = 35 \pm 14\ M^{-1}\ s^{-1}$$

These rate constants indicate that the H_3L^- species does indeed react faster than the H_2L^{2-} species. Despite the H_3L^- species being present as an intermediate, the H_2L^{2-} species is the primary intermediate observed. NMR and X-ray studies show that the two protons of the H_2L^{2-} intermediate are in a *trans* configuration (Figure 5).[11] Both steric and electron repulsion hamper the completion of the final chelate.

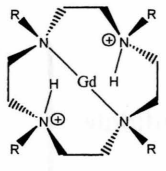

Acetate groups not shown for clarity

Figure 5: *trans* H_2L^{2-} intermediate

The dissociation also proceeds at a favorably slow rate. Experimental results indicate that this first order rate law depends

only on the proton concentration, $[H^+]$.[11] The rate constant for dissociation, k_d, thus follows the rate law

$$k_d = k_{d,0} + k_{d,H}[H^+] \qquad (11)$$

The rate of dissociation is on a time scale of days, not hours as observed with open ligands. The rate constant, $k_{d,0}$ has a value of zero within experimental error. The mechanism of dissociation is not known at the present time. Researchers have postulated that a proton binds into the primary coordination sphere of the complex. For the ligand to dissociate from the metal, the proton of [HGd(DOTA)] must rearrange and protonate an amine nitrogen, essentially forming the HL^{3-} species previously seen. The rigid macrocyclic cage prevents this rearrangement from occurring at any appreciable rate. Experiments[2] have shown that a more rigid group attached to the ring hampers dissociation even further. A CH_2 group on the ligand (CY)DOTA (Figure 6) has been replaced by a cyclohexane ring. This added rigidity nearly doubles the Gd-complex's half-life. By adjusting the DOTA ligand in this way, the relaxivity remains unaffected while the toxicity is greatly reduced.

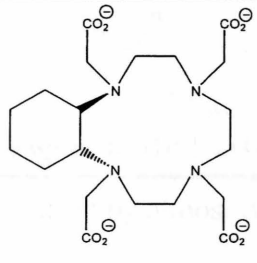

Figure 6: (CY)DOTA

Derivatives of the DOTA Ligand

The idea of modifying the DOTA ligand to give added stability or increased relaxivity has yielded many new and interesting potential contrast agents.[1,2,5,11-13] The first modified DOTA derivative ligand appeared in 1991.[12] By replacing one acetate pendant arm with a hydrogen, the DO3A ligand (Figure 7)

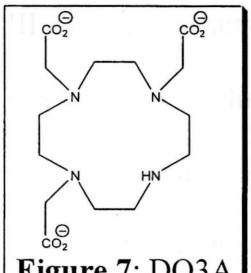

Figure 7: DO3A

allows a second water molecule to coordinate the Gd(III). While obviously increasing the relaxivity of the complex, [Gd(DO3A)] became the first neutral macrocyclic Gd(III) complex. A neutral complex is required to cross the blood-brain barrier.[1] Also, a concentrated injection of charged complex is hyperosmolar to blood and tissue and causes pain to the patient.[12] Surprisingly, [Gd(DO3A)] has a high level of thermodynamic stability. The rigid cyclen backbone also provides a high level of kinetic inertness.[12]

Additional functionality can be added to the DO3A ligand through reactions with the N-H group. Almost immediately after the discovery of DO3A, a synthesis of the more stable HP-DO3A (Figure 8) arose.[1] For this ligand, the N-H group is replaced with a 2-hydroxypropyl group. The hydroxy group remains protonated under physiological conditions which causes the [Gd(HP-DO3A)] complex to be overall neutral. Since the thermodynamic stability of this ligand is raised by almost two-log units over [Gd(DO3A)], research into [Gd(DO3A)] has effectively ceased.[1] The relaxivity of [Gd(HP-DO3A)], however, is lower than that of [Gd(DO3A)]. Detailed kinetic studies into the complex have only recently been reported.[14] In the United States, the [Gd(HP-DO3A)] complex has passed Phase I, II and III trials and awaits final governmental approval. European countries have already put this complex to clinical use.[1]

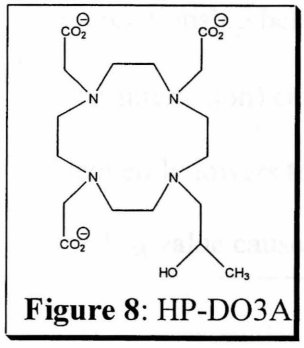

Figure 8: HP-DO3A

Macromolecular Studies

The ability to manipulate the N-H group creates the possibility of easily linking multiple ligands into one macromolecule.[2] The simplest approach is to link two DO3A

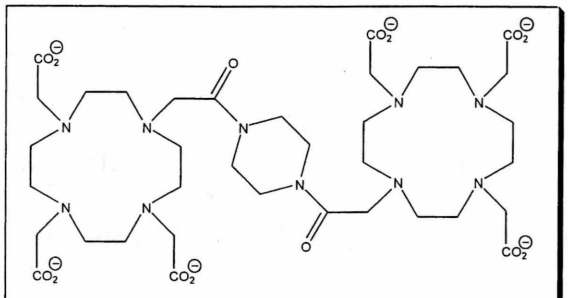

Figure 9: PIP-bis(DO3A)

ligands together. The increased molecular weight of the resulting dimer, PIP-bis(DO3A), (Figure 9)[15] has a profound effect on the relaxivity of the complex. The Solomon-Bloembergen-Morgan theory[16] (Equations (2)-(5), chapter I) explains the reason for creating high molecular weight complexes. The high molecular weight slows the overall rotation tumbling time of the entire complex. Also, the rigid nature of the complex reduces the motion of each Gd-chelate. This restriction of movement lowers the τ_R (rotational tumbling) variable. The direct relationship between τ_R and τ_c (the correlation time for the modulation of the dipolar interaction) causes a decrease in the value of τ_c. The decreased value of τ_c subsequently lowers the value of T_{1M} (the longitudinal proton relaxation time). The lower T_{1M} value causes an increase in R_{1p}^{is}, i.e. a higher relaxivity.

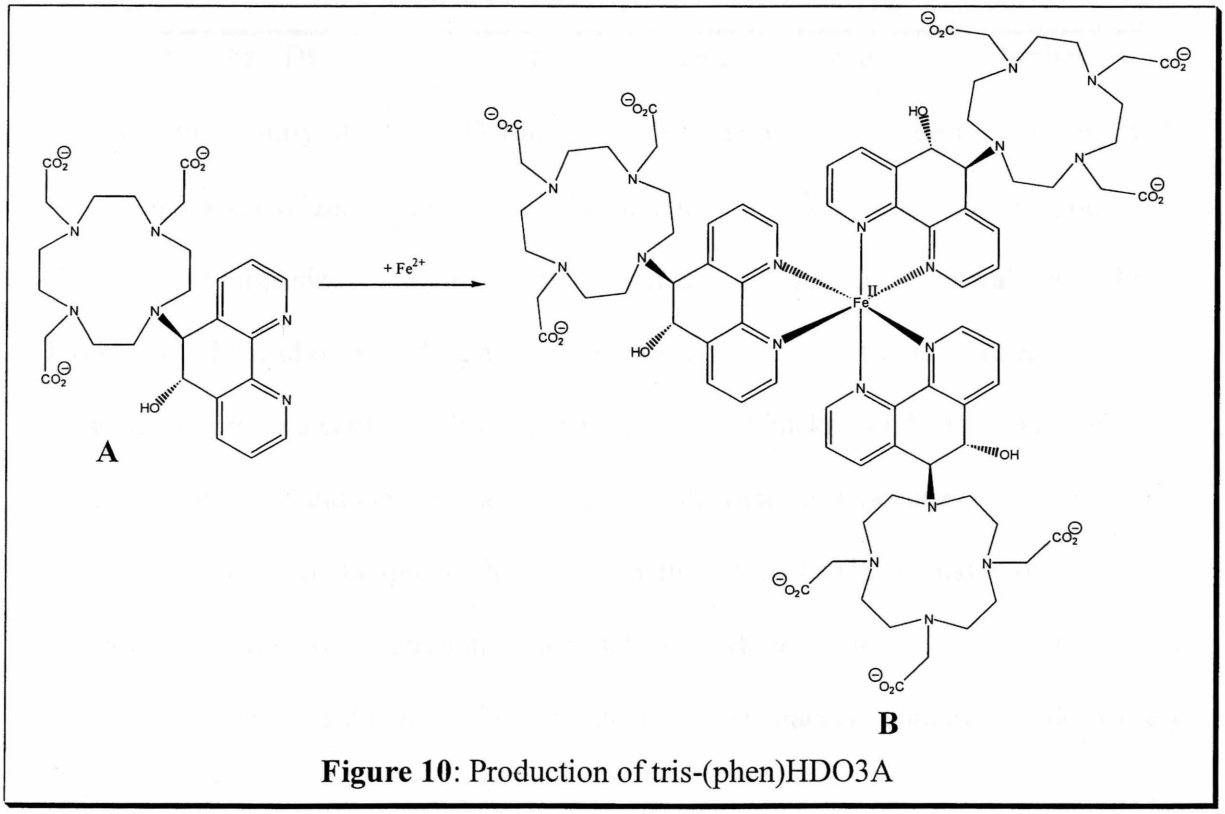

Figure 10: Production of tris-(phen)HDO3A

A second, unique method of creating a macromolecule is shown by the ligand (phen)HDO3A (Figure 10A).[2] This ligand can bind two different metals by exploiting two different binding sites. The macrocyclic site complexes Gd(III) in a stable fashion while the phenanthroline-like site easily binds Fe(II) to create a high molecular weight tris-complex (Figure 10B).

A third method of achieving high molecular mass complexes involves the attachment of Gd-complexes to dendrimers.[13] The basic characteristic of a dendrimer is a highly ordered three-dimensional star polymer. A promising example of this is

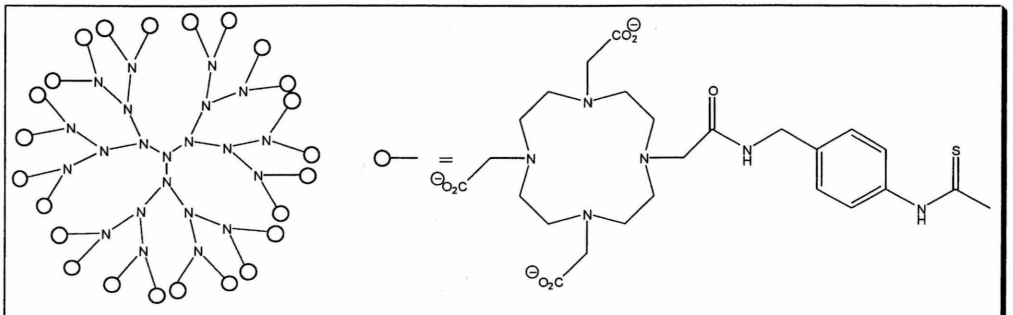

Figure 11: [G3{N[CS]N-bz-{DO3A}$_{23}$]

[G3(N[CS]N-bz-{DO3A}$_{23}$] (Figure 11). The three-dimensional polymer further increases the rigidity of each DO3A linkage, which helps to lower the τ_R variable. With an overall charge of zero, the dendrimer has potential use as a blood pool imaging agent.[17] The large size of the three-dimensional structure prevents removal out of the blood pool. Instead of providing a contrast between cancerous tissue and healthy tissue, these agents create a contrast between blood and serum background. This can help elucidate pathways and may be used to locate cardiovascular blockages.

The ability to manipulate the basic structure of the DOTA ligand allows for a magnificent amount of research into potential uses. Manipulations can yield products of varying relaxivity and stability. These products can be attached to an even wider variety

of compounds to create macromolecular complexes that give even better relaxivity. Despite such a plethora of interesting options to explore with the DOTA ligand, many research groups have focused on potential contrast agents unrelated to the DOTA ligands. When designing these new ligands, researchers attempt to use entirely new ideas and theories to increase both relaxivity and stability. Some of these new complexes also open new areas of uses for contrast agents. The next chapter will explore two of these new classes of complexes.

References

[1] Reichert, D. E.; Lewis, J. S.; Anderson, C. J. "Metal Complexes as Diagnostic Tools." *Coord. Chem. Rev.* **1999**, *184*, 3-66.

[2] Comblin, V.; Gilsoul, D.; Hermann, M.; Humblet, V.; Jacques, V.; Mesbahi, M.; Sauvage, C.; Desreux, J. F. "Designing new MRI Contrast Agents: A Coordination Chemistry Challenge." *Coord. Chem. Rev.* **1999**, *185-186*, 451-470.

[3] Sandes, R. W.; Vasilevskis, T. J.; Undheim, K.; Gacek, M. WO Patent 96/28432. 1996.

[4] Argese, M.; Ripa, G.; Scala, A.; Valle, V. WO Patent 97/49691. 1997.

[5] Parker, D.; Williams, J. A. G. "Getting Excited About Lanthanide Complexation Chemistry." *J. Chem. Soc., Dalton Trans.* **1996**, 3613-3628.

[6] Desreux, J. F. "Nuclear Magnetic Resonance Spectroscopy of Lanthanide Complexes with Tetraacetic Tetraaza Macrocycle. Unusual Conformation Properties." *Inorg. Chem.* **1980**, *19*, 1319-1324.

[7] Spirlet, M. R.; Rebizant, J.; Desreux, J. F.; Loncin, M. F. "Crystal and Molecular Structure of Sodium Aquo(1,4,7,10-tetraazacyclododecane-1,4,7,10-tetraacetato)europate(III) Tetrahydrate, Na^+ $(EuDOTAI \cdot H_2O)^- \cdot 4H_2O$, and Its Relevance to NMR Studies of the Conformational Behavior of the Lanthanide Complexes Formed by the Macrocyclic Ligand DOTA." *Inorg. Chem.* **1984**, *23*, 359-363.

[8] Amie, S.; Botta, M.; Ermondi, G. "NMR Study of Solution Structure of Lanthanide(III) Complexes of DOTA." *Inorg. Chem.* **1992**, *31*, 4291-4299.

[9] Dunand, F. A.; Aime, S.; Merbach, A. E. "First ^{17}O NMR Observation of Coordinated Water on Both Isomers of $[Eu(DOTAM)(H_2O)]^{3+}$: A Direct Access to Water Exchange and it Role in the Isomerization." *J. Am. Chem. Soc.* **2000**, *122*, 1506-1512.

[10] Aime, S.; Botta, M.; Fasano, M.; Marques, M. P. M.; Geraldes, C. F. G. C.; Pubanz, D.; Merbach, A. E. "Conformational and Coordination Equilibria on DOTA Complexes of Lanthanide Metal Ions in Aqueous Solution by ^1H-NMR Spectroscopy." *Inorg. Chem.* **1997**, *36*, 2059-2068.

[11] Wang, X.; Jin, T.; Comblin, V.; Lopez-Mut, A.; Merciny, E.; Desreux, J. F. "A Kinetic Investigation of Lanthanide DOTA Chelates. Stability and Rates of Formation and of Dissociation of a Macrocyclic Gadolinium (III) Polyaza Polycarboxylic MRI Contrast Agent." *Inorg. Chem.* **1992**, *31*, 1095-1099.

[12] Dischino, D. D.; Delaney, E. J.; Emswiler, J. E.; Gaughan, G. T.; Prasad, J. S.; Srivastava, S. K.; Tweedle, M. F. "Synthesis of Nonionic Gadolinium Chelates

Useful as Contrast Agents for Magnetic Resonance Imaging. 1,4,7-Tris(carboxymethyl)-10-substituted-1,4,7,10-tetraazacyclododecanes and Their Corresponding Gadolinium Chelates." *Inorg. Chem.* **1991**, *30*, 1265-1269.

[13] Toth, E.; Pubanz, D.; Vauthey, S.; Helm, L.; Merbach, A. E. "The Role of Water Exchange in Attaining Maximum Relaxivities for Dendrimeric MRI Contrast Agents." *Chem. Eur. J.* **1996**, *2*, 1607-1615.

[14] Bianchi, A.; Calabi, L.; Giorgi, C.; Losi, P.; Mariani, P.; Paoli, P.; Rossi, P.; Valtancoli, B.; Virtuani, M. "Thermodynamic and Structural Properties of Gd3+ Complexes with functionalized macrocyclic ligands based upon 1,4,7,10-tetraazacyclododecane." *J. Chem. Soc., Dalton Trans.* **2000**, 697-705.

[15] Yam, V. W. W; Lo, K. K. W. "Recent Advances in Utilization of Transition Metal Complexes and Lanthanides as Diagnostic Tools." *Coord. Chem. Rev.* **1999**, *184*, 157-240.

[16] Lauffer, R. B. "Paramagnetic Metal Complexes as Water Proton Relaxation Agents for NMR Imaging: Theory and Design." *Chem. Rev.* **1987**, *87*, 901-927.

[17] Bogdanov, A.; Weissleder, R.; Brady, T. J. "Long-Circulating Blood Pool Imading Agents." *Adv. Drug Delivery Rev.* **1995**, *16*, 335-348.

Chapter III

Recent Advances in Contrast Agent Technology

Typically, improvements in the relaxivity effects of a contrast agent have come at the cost of stability to the contrast agent. Many research groups have focused on novel solutions to increase relaxivity while not sacrificing complex stability by studying Gd(III) complexes unrelated to the $[Gd(DOTA)]^-$ complex. Two of the more interesting and successful ligands are presented here. The first ligand presented, the texaphyrin ligand, has the ability to complex lanthanide series metals in a 1:1 near in-plane fashion. Moving away from the macrocyclic cage binding seen in all DOTA-like Gd(III) complexes greatly improves the water exchange dynamics. The second ligand presented, PCTA, remains faithful to the macrocyclic cage approach but also introduces pyridine functionality into the macrocycle ring. The addition of the pyridine moiety strengthens the stereochemical rigidity of Gd(III) complexes. This added stability allows more water coordination sites on the metal, thus increasing the relaxivity.

The $[Gd(Texaphyrin)]^{2+}$ Contrast Agent

To craft a ligand capable of binding a lanthanide series metal in a 1:1 near in-plane fashion, Sessler[4] et al. looked to natural metal binding macrocycles. The most common natural metal binding macrocycle is the porphyrin ring (Figure 1). Various forms of the porphyrin ring exist and bind transition metals in a 1:1 planar fashion in a number of complexes including heme in hemoglobin and cytocrome P_{450}. The porphyrin ring can express different traits depending on what substituent groups reside along the exterior of the ring. Some tumors selectively uptake different porphyrin complexes.[1] This selective uptake can be exploited to help create a contrast. Many metal

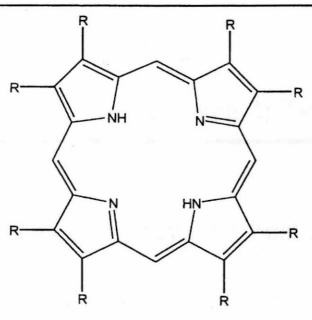

Figure 1: Porphyrin Ring

porphyrins remain in tumor cells for more than four days.[1] Lanthanide-porphyrin complexes, however, dissociate rapidly under mild conditions.[2] The increased size of the trivalent lanthanide ion is too large for the porphyrin-binding cavity. The metal cannot form a stable 1:1 complex but rather forms a dimeric 2:1 or 3:2 sandwich structure. To alleviate this problem, considerable research has been directed towards expanding the binding cavity of the porphyrin macrocycle.

One such class of expanded porphyrin macrocycles is the texaphyrins (Figure 2). Replacement of one pyrrole ring with two Schiff base nitrogens creates a binding cavity about 20% larger while maintaining aromaticity.[3] The five ligating nitrogens (three pyrrole and two Schiff base) form a stable 1:1 near in-plane complex with almost all lanthanide series ion. Much like porphyrin rings themselves, the substituents on each of the pyrrole rings and the substituents on the phenyl ring can be varied. This allows for a wide variety of ligands with different properties. A Gd(III) complex with the ligand shown in Figure 2 displays the best relaxivity and therefore has the greatest potential as an MRI contrast agent.[4,5]

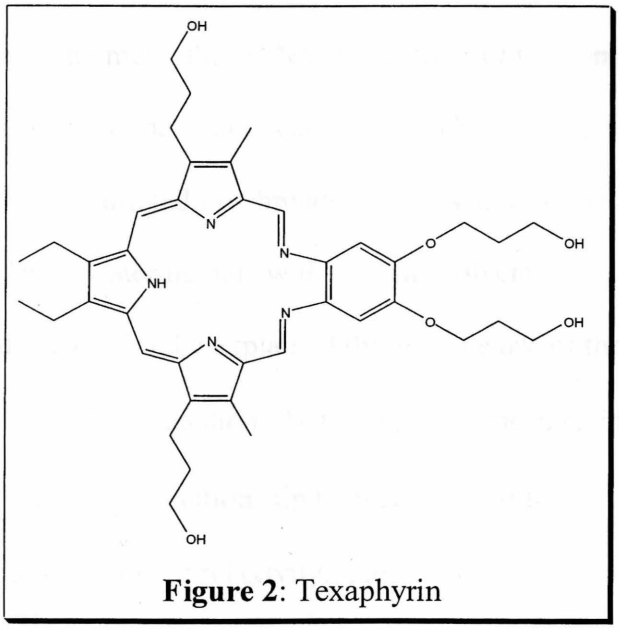

Figure 2: Texaphyrin

Crystallographic data of $[Gd(Texaphyrin)]^{2+}$ suggests that the complex forms both a nine coordinate species and a ten coordinate species.[5] The ability of

$[Gd(Texaphyrin)]^{2+}$ to axially bind four to five water molecules into the inner coordination sphere of Gd(III) is the reason for such a high level of relaxivity.[3] Solomon-Bloembergen-Morgan theory[6] (Equations (2)-(5), chapter I) shows a direct relationship between q (the number of bound water molecules) and relaxivity, R_{1p}^{is}. These additional directly bound waters help to increase relaxivity 3-4 times over current contrast agents such as $[Gd(DOTA)]^{-}$.[4] Researchers measured the longitudinal relaxivity, R_1, to be 16.9 $\pm$ 1.5 mM^{-1} s^{-1} at 50 MHz.[2,4]

Axial ligation studies have begun to elucidate why $[Gd(Texaphyrin)]^{2+}$ displays such a high level of relaxivity.[3] A study was performed on both paramagnetic and diamagnetic complexes of the texaphyrin ligand in a methanol medium. In a comparison measurement, the ^1H NMR spectrum of the complex in an aqueous medium shows the axially bound water peak to have a broader signal than the axially bound methanol peak. This additional line broadening presumably comes from the faster exchange of the axially bound water ligands with the bulk solvent water. Again, the relaxivity effect of solvent diffusion can be explained through the use of the Solomon-Bloembergen-Morgan theory.[6] In equation (2), the τ_M is the mean residence lifetime of the axially bound water. The inverse relationship between τ_M and R_{1p}^{is} indicates that a lower residence lifetime causes a higher relaxivity. Fast exchange of the axially bound water ligand with the bulk solvent water leads to a lower resident lifetime of the bound water.

This high level of relaxivity remains constant for approximately four days.[5] This longevity can only mean a high level of *in vitro* stability. An initial study of $[Gd(Texaphyrin)]^{2+}$ with freshly drawn blood plasma at physiological temperature gave no measurable degradation after 5-h.[4] This encouraging result means the complex is

potentially stable *in vivo*. Before any *in vivo* studies could occur, *in vitro* binding of Gd(III) to the texaphyrin ligand had to be rigorously studied.[5] The complex was placed in an aqueous medium along with three other complexing agents: EDTA (which readily complexes with Gd(III)), oxalate and phosphate (both of which form water insoluble complexes). UV/vis measurements of λ_{max} peaks of Soret and Q-type bands were used to measure the Gd(III) texaphyrin complex. A rapid decrease in the intensity of each band was seen, but no change in position was observed. This puzzling result prompted researchers to perform a second experiment. The $[Gd(Texaphyrin)]^{2+}$ complex was again placed in an aqueous medium but with only EDTA as a competing complexing agent. After one week of sitting in a dark room, the same results were obtained. FAB Mass Spectrometry of the green solution showed a peak corresponding to only the $[Gd(Texaphyrin)]^{2+}$ and no free macrocycle. The solution was allowed to sit for a 45-day period. Again, no shift in the UV/vis spectra could be seen. The only conclusion can be that the rapid drop of intensity cannot be from demetalation. The complex is stable at a pH of 7 in the presence of EDTA for long periods of time. Studies show that the rate of drop is only dependent on the concentration of complex and not of EDTA. One hypothesis as to the reduced intensity of the bands relates to the ability of porphyrin rings to aggregate in aqueous solution.[5] Possibly, the complex quickly aggregates together. This would reduce the intensity signal of the complex while not necessarily changing the position of the peak. If the aggregation of complex did not affect the metal center, then no noticeable shift in peak position would be seen. The reason for this UV/vis result is not truly understood. It was not considered pertinent to the contrasting ability of the complex, therefore no additional testing was performed.[5]

The positive *in vitro* studies encouraged researchers to begin *in vivo* animal-imaging studies. One rabbit study showed that an enhanced tumor image could be rendered with injections as low as 5 μmol/kg.[2] A liver image could be achieved with only 2 μmol/kg. Studies on the toxicity of the complex in rats also showed very favorable results. Rats administered 20 μmol/kg daily for 21 days showed no signs of toxicity.[2,4] The clinical doses initially appear to be safe and effective. In addition to requiring such low doses, the enhanced image remained for about 3.5 hours.[4] This presents a vast improvement over current MRI contrast agents. Current MRI contrast agents aggregate in the kidneys and cannot image tumors after only a few minutes. Despite already showing this improved relaxivity over current contrast agents, researchers aim to further enhance the relaxivity of texaphyrin based contrast agents.

The synthetic scheme for the texaphyrins allows for a broad and varied approach to improving relaxivity. One approach is to create a water soluble dimer of the

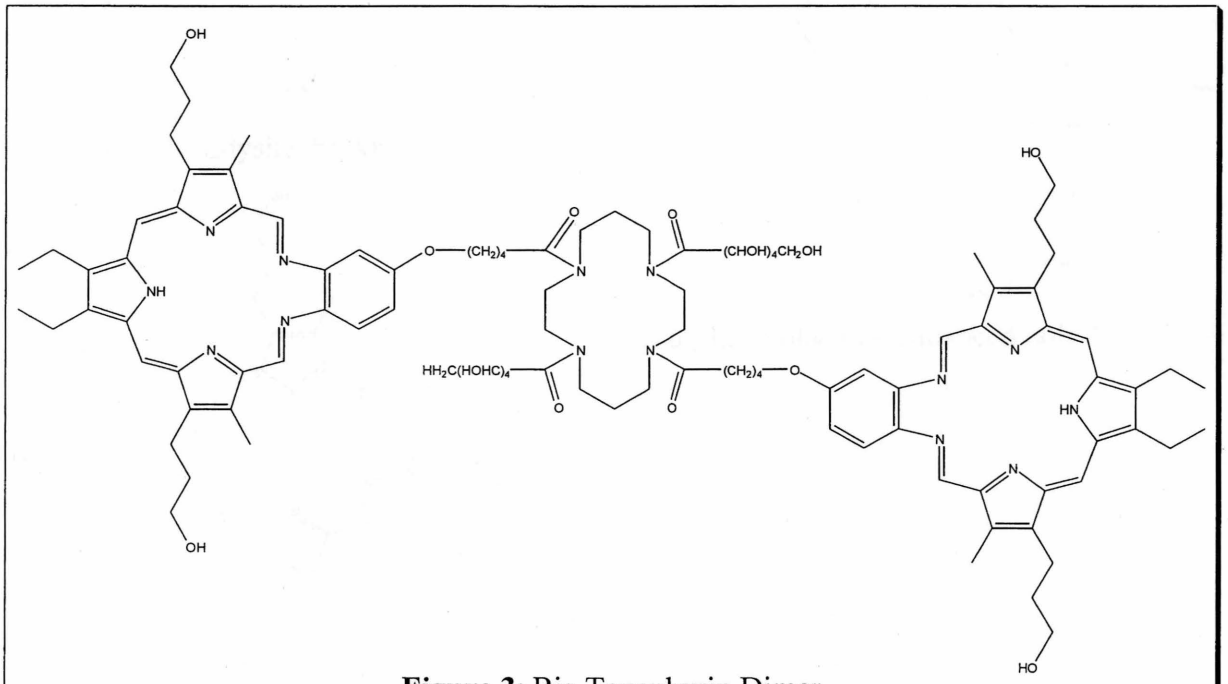

Figure 3: Bis-Texaphyrin Dimer

texaphyrin ligand (Figure 3).[7] The creation of dimers reduces both the rotational tumbling and molecular freedom of the complex. As indicated by the Solomon-Bloembergen-Morgan theory[6], this reduces the rotational tumbling variable, τ_R. The lower τ_R value increases the relaxivity. This dimer has been shown to have a T_1 relaxivity of 40 mM^{-1} s^{-1} at 500 MHz, neutral pH and room temperature. In contrast, note that $[Gd(Texaphyrin)]^{2+}$ displays only 8 mM^{-1} s^{-1} under the same conditions and $[Gd(DOTA)]^-$ only about 4 mM^{-1} s^{-1}.[7,8] This particular bridging ligand also has the potential of binding a third metal species.[7]

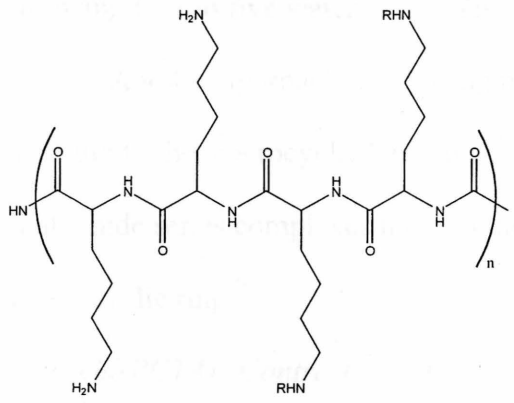

A: Poly-L-lysine backbone

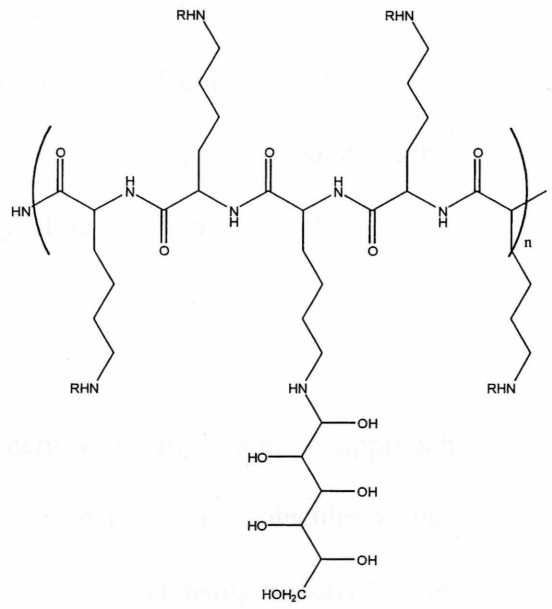

B: δ-gluconolactone enhanced poly-L-lysine backbone

R =

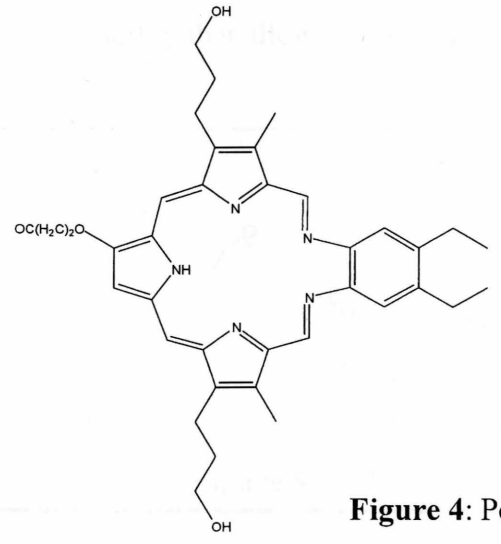

Figure 4: Polymeric Texaphyrin Systems

Improved relaxivity can also be achieved through the addition of the texaphyrin ligand to a polymer chain. The addition to poly-L-lysine (Figure 4A) improved relaxivity to 90 mM^{-1} s^{-1} at 500 MHz, neutral pH and room tempertature.[7] A reaction with δ-gluconolacetone functionalizes the polymer backbone (Figure 4B). This added functionality produces increased relaxivity to 315 mM^{-1} s^{-1} under the same conditions.

The $[Gd(Texaphyrin)]^{2+}$ complex represents a new strategy to enhance the relaxivity of MRI contrast agents. Using the natural metal binding porphyrin as a template for creating expanded porphyrin macrocycles, Sessler created the first near in-plane 1:1 lanthanide series complex. This complex shows increased relaxivity by allowing four to five water molecules to bind axially to the Gd(III) ion.

Another approach to allowing more coordinated water molecules is to add strength to the macrocyclic backbone. The PCTA class of ligands gives added strength to lanthanide series complexes through the addition of pyridine functionality to the macrocyclic ring.[9]

The [Gd(PCTA)] Contrast Agent

The addition of pyridine functionality to the macrocyclic ring is a novel approach to added stability that allows for a greater number of coordinated water molecules while also not increasing toxicity.[10] This strategy of incorporating a pyridine ring into the macrocycle has yielded a variety of different PCTA (*P*yridine-*C*ontaining *T*riaza Macrocyclic Tri*A*cetate) ligands.

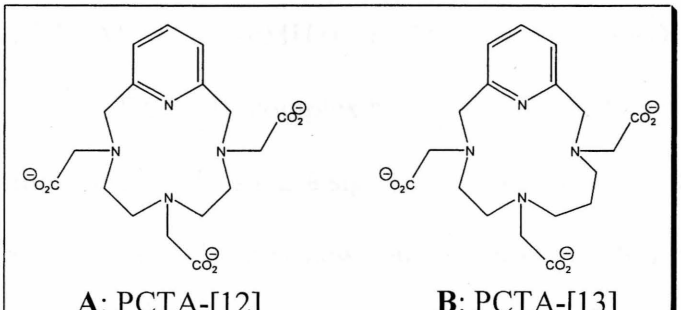

A: PCTA-[12] **B**: PCTA-[13]

Figure 5: PCTA

Two such ligands show promise as MRI contrast agents when complexed with Gd(III).[10-13] The PCTA-[12] (Figure 5A) ligand contains a triaza 12-member ring while PCTA-[13] (Figure 5B) contains a triaza 13-member ring.[10] The size of each ring cavity forces the Gd(III) ion to rest above the plane of the ring. The pendant acetate arms wrap around the metal in a [Gd(DOTA)]$^-$-like fashion. As with [Gd(DOTA)]$^-$, the pendant acetate arms wrap in two different fan-like directions (Figure 6).[12] The increased stability due to the addition of the pyridine moiety to the ring reduces conformational changes between the two states. How this affects relaxivity is unknown at this time. Despite binding lanthanide ions in a similar macrocyclic cage fashion as the DOTA ligand, the PCTA ligands show very different kinetics of formation.[9] Metal complexation proceeds at a much faster rate and no MH_XL intermediate species has been observed.

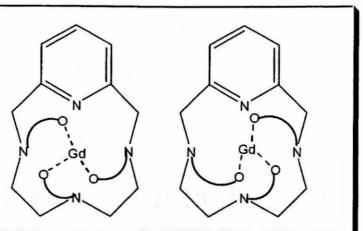

Figure 6: Conformations of the [Gd(PCTA)] complex

The increased stability provided by the pyridine ring allows PCTA to form a stable Gd(III) complex while only donating seven binding ligands (three tertiary amine nitrogens, one pyridine nitrogen, and three acetate oxygens).[10] This allows two water molecules to enter into the inner coordination sphere of the Gd(III). The two inner coordinated water molecules increase the relaxivity of the [Gd(PCTA-[13])] complex (7.7 mM^{-1} s^{-1} at 20 MHz)[13] by 35% over the [Gd(DOTA)]$^-$ complex.[12] Also, the [Gd(PCTA-[13])] complex has a larger secondary coordinated sphere of water molecules.[13] This has a significant contribution to the overall relaxivity of the complex.

This relatively new complex lies at the frontier of contrast agent technology. This ligand and Gd(III) complexes of the ligand have not been studied with the same depth or

intensity as the $[Gd(DOTA)]^-$ complex. One of the more interesting potential applications of the [Gd(PCTA)] class of complexes is as an organ/tissue specific contrast agent.[9] Unlike the DOTA ligand, modifications of the PCTA pyridine ring allow the addition of functionality without changing the binding nature of the ligand. This fact allows various functional groups to be added while not affecting the stability of the complex. One such functional group attempts to link PCTA-[12] to a macromolecule.[14] The addition of the bromo-benzyloxy group yields the BB-PCTA-[12] (Figure 7) ligand, which gives the necessary functionality to successfully link the [Gd(PCTA-[12])] complex to a macromolecule. It is hoped that a macromolecular system based on PCTA technology will be more successful than one based on DOTA technology. The desired effects of lowering the τ_R (rotational tumbling constant) value has been shown to be quenched by relatively long τ_M (mean residence lifetime of the bound water) values. By restricting the molecular freedom of the $[Gd(DOTA)]^-$ complex, a slower rate of conformational change is seen. Subsequently, the bound water resides on the Gd(III) for a longer period of time, thus reducing the relaxivity effects. The ability of the [Gd(PCTA-[12])] complex to bind two water molecules offsets this quenching effect.[14]

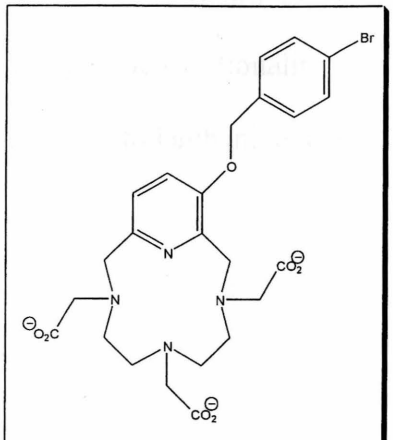

Figure 7: BB-PCTA-[12]

The two classes of ligands presented in this chapter show the forefront of contrast agent technology. Each of these complexes increases both the relaxivity and the stability of the contrast agent. The next chapter will deal with research done in the Uffelman group. Ligands produced in the Uffelman group combine many ideas seen in these two

successful ligands. First, the binding cavity of our ligands are close to the size of the texaphyrin binding cavity. We hope that our ligand will also bind lanthanide series metals in a near in-plane fashion. Secondly, the ligand design centers on the introduction of pyridine functionality to the macrocyclic ring. We hope this will add strength and stability to lanthanide metal complexes.

References

[1] Matthews, S. E.; Pouton, C. W.; Threadgill, M. D. "Macromolecular Systems for Chemotherapy and Magnetic Resonance Imaging." *Adv. Drug Delivery Rev.* **1996**, *18*, 219-267.

[2] Sessler, J. L.; Hemmi, G.; Mody, T. D.; Murai, T.; Burrell, A.; Young, SW. "Texaphyrins: Synthesis and Application." *Acc. Chem.* **1994**, *27*, 43-50.

[3] Lisowski, J.; Sessler, J. L.; Lynch, V.; Mody, T. D. "^{1}H NMR Spectroscopic Study of Paramagnetic Lanthanide(III) Texaphyrins. Effect of Axial Ligation." *J. Am. Chem. Soc.* **1995**, *117*, 2273-2285.

[4] Sessler, J. L.; Mody, T. D.; Hemmi, G. W.; Lynch, V.; Young, S. W.; Miller, R. A. "Gadolinium(III) Texaphyrin: A Novel MRI Contrast Agent." *J. Am. Chem. Soc.* **1993**, *115*, 10368-10369.

[5] Sessler, J. L.; Mody, T. D.; Hemmi, G. W.; Lynch, V. "Synthesis and Structural Characterization of Lanthanide(III) Texaphyrins." *Inorg. Chem.* **1993**, *32*, 3175-3187.

[6] Lauffer, R. B. "Paramagnetic Metal Complexes as Water Proton Relaxation Agents for NMR Imaging: Theory and Design." *Chem. Rev.* **1987**, *87*, 901-927.

[7] Sessler, J. L.; Kral, V.; Hoehner, M. C.; Chin, K. O. A.; Davila, R. M. "New Texaphyrin-type expanded porphyrins." *Pure and Appl. Chem.* **1996**, *68*, 1291-1295.

[8] Comblin, V.; Gilsoul, D.; Hermann, M.; Humblet, V.; Jacques, V.; Mesbahi, M.; Sauvage, C.; Desreux, J. F. "Designing new MRI Contrast Agents: A Coordination Chemistry Challenge." *Coord. Chem. Rev.* **1999**, *185-186*, 451-470.

[9] Kim, W. D.; Hrncir, D. C.; Kiefer, G. E.; Sherry, A. D. "Synthesis, Crystal Structure, and Potentiometry of Pyridine-Containing Tetraaza Macrocyclic Ligands with Acetate Pendant Arms." *Inorg. Chem.* **1995**, *34*, 2225-2232.

[10] Aime. S.; Botta, M.; Crich, S. G.; Giovenzana, G. B.; Jommi, G.; Pagliarin, R.; Sisti, M. "Synthesis and NMR Studies of Three Pyridine-Containing Triaza Macrocyclic Triacetate Ligands and Their Complexes with Lanthanide Ions." *Inorg. Chem.* **1997**, *36*, 2992-3000.

[11] Kim, W. D.; Kiefer, G. E.; Maton, F.; McMillan, K.; Muller, R. N.; Sherry, A. D. "Relaxometry, Luminescence Measurements, Electrophoresis, and Animal Biodistribution of Lanthanide(III) Complexes of Some Polyaza Macrocyclic Acetates Containing Pyridine." *Inorg. Chem.* **1995**, *34*, 2233-2243.

[12] Amie, S.; Botta, M.; Crich, S. G.; Giovenzana, G. B.; Jommi, G.; Pagliarin, R.; Sisti, M. "MRI Contrast Agents: Macrocyclic Lanthanide(III) Complexes with Improved Relaxation Efficiency." *J. Chem. Soc., Chem. Commun.* **1995**, 1885-1886.

[13] Amie, S.; Botta, M.; Crich, S. G.; Giovenzana, G. B.; Jommi, G.; Pagliarin, R.; Piccinini, M.; Sisti, M.; Terreno, E. "Towards MRI contrast agents of improved efficacy. NMR relaxometric investigations of the binding interaction to HSA of a novel heptadentate macrocyclic triphosphonate Gd(III)-complex." *J. Bio. Inorg. Chem.* **1997**, *2*, 470-479.

[14] Aime, S.; Botta, M.; Frullano, L.; Crich, S. G.; Giovenzana, G. B.; Pagliarin, R.; Palmisano, G.; Sisti, M. "Contrast Agents for Magnetic Resonance Imaging: A Novel Route to Enhanced Relaxivities Based on the Interaction of a Gd^{III} Chelate with Poly-β-cyclodextrins." *Chem. Eur. J.* **1999**, *5*, 1253-1260.

Chapter IV

The Uffelman Group

Ligand design in the Uffelman group does involve many theories and ideas seen previously in this thesis. Specifically, the group hopes to achieve a 1:1 near in-plane binding of a lanthanide series ion to a pyridine containing macrocycle. All ligands discussed thus far (DOTA[1], texaphyrin[2], and PCTA[3]) use amine nitrogens to bind the lanthanide ion. Currently in coordination chemistry, no ligand uses an amido-N nitrogen to bind a lanthanide series ion. Through careful design, we hope to expand the coordination of lanthanide ions to amido-N ligands. Our lab has completed one macrocyclic ligand and is currently close to completing a second. These two ligands expand upon earlier research in the group that provided insightful results while not actually creating a viable ligand.

Background Research

Early research in the group attempted to expand the macrocyclic cavity of previously created ligands.[4,5] This tetradentate ligand (Figure 1A)[4] created under Collins and Uffelman has been shown to bind transition metals effectively. It was thought that replacing the diethyl malonyl group with a 2,6-pyridine dicarbonyl group would increase the cavity size while also adding a fifth coordination site. The proposed molecule (Figure 1B) was successfully synthesized but proved too

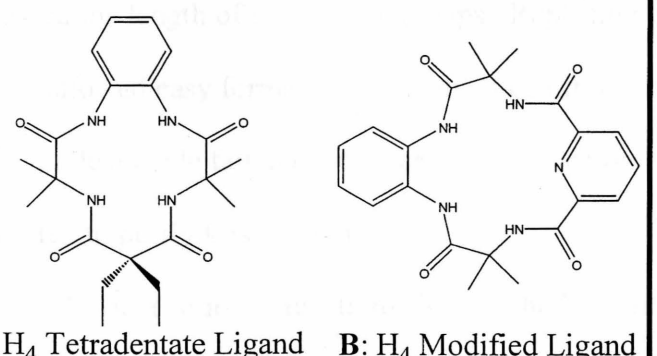

A: H_4 Tetradentate Ligand **B**: H_4 Modified Ligand

Figure 1: Previous Ligands

insoluble to purify. It is thought that intermolecular H-bonding and π-stacking of this relatively flat molecule leads to this insolubility.

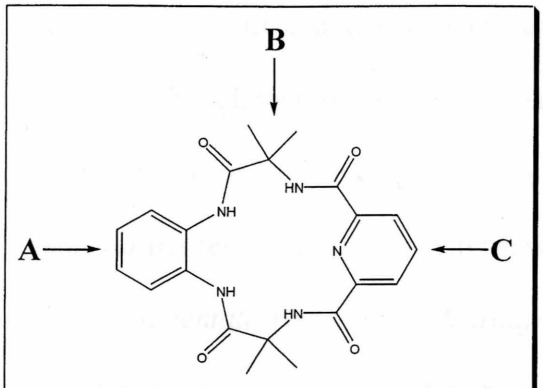

Figure 2: Proposed Modifications

Three conceptual methods were proposed to increase ligand solubility. The first possible change involved a change to the substituents of the phenyl ring (Figure 2A). Depending on the group added, this addition would change both the solubility and electronic properties of the ligand. A second change was a modification of the alkyl R groups (Figure 2B). The proposed change would alter the solubility and sterics of the ligand while not appreciably changing the electronics. The third change involved the addition of substituents to the pyridine ring (Figure 2C). This would have effects on both the solubility and the electronic properties. Due to cumbersome procedures, this method has not yet been explored.

The first attempts to increase the solubility employed the second method and increased the length of the alkyl R groups. Replacing the methyl groups with propyl groups allowed easy formation of the diamide dibromide intermediate. Reactions to form the diamide diazide failed to produce a clean reaction. No further research has been attempted to purify this reaction.

The next series of reactions used method one in an attempt to create a dialkoxy phenylenediamine (Figure 3). This molecule was successfully synthesized but decomposed too quickly to be currently

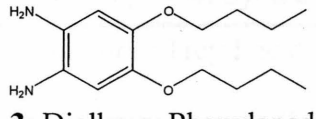

Figure 3: Dialkoxy Phenylenediamine

incorporated into the total synthesis of a macrocycle. It was thought that extreme air sensitivity caused the rapid decomposition. This reaction has also been temporarily abandoned. At the time students conducted this reaction, the Uffelman lab did not have a inert atmosphere glove box. Since then, a new glove box equipped to perform reactions and remove solvent without ever exposing the reactants to air has been purchased. Perhaps further research into this will prove fruitful.

The H_4 Pentadentate Tetraamide Macrocycle

A radical change in procedure brought on the first successful ligand design. This new direction involved a change in the production of the diamide diamine intermediate.[6]

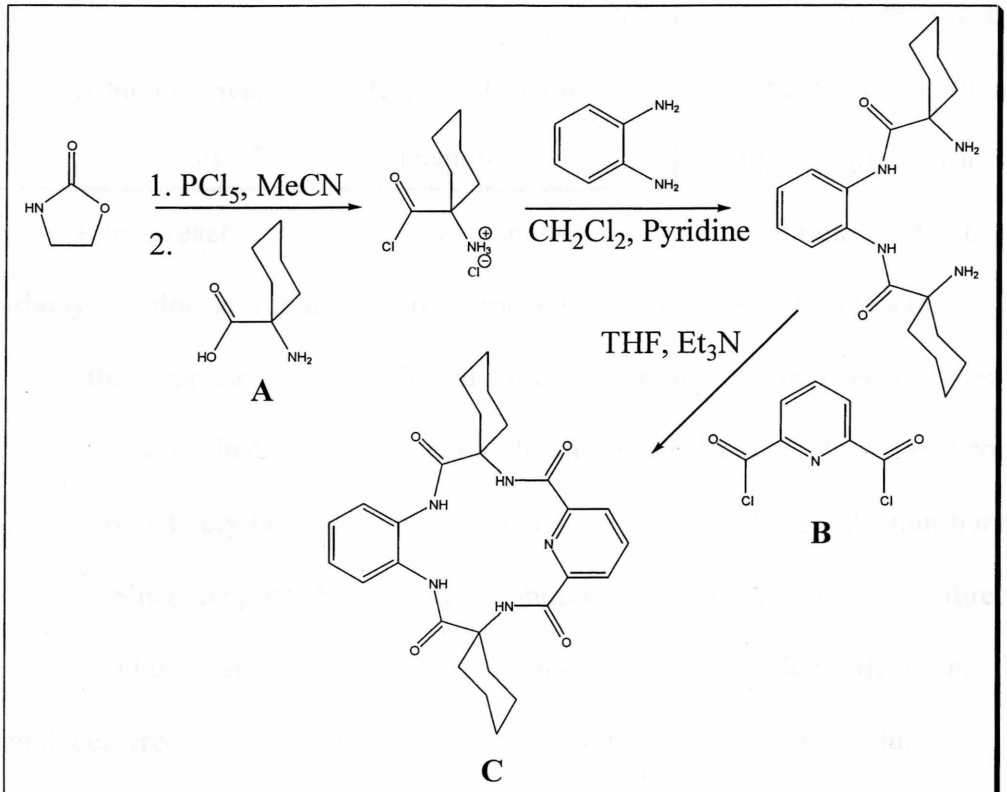

Figure 4: Synthesis of H_4 Pentadentate Macrocycle

Former group member Trey Lee developed a synthesis[7] (Figure 4) that no longer proceeded through the diamide diazide. This new synthesis used a commercially inexpensive amino acid starting material. This meant that the alkyl R group could now

be modified easily. Lee first attempted this new synthesis using 1-amino-1-cyclohexane carboxylic acid (Figure 4A). This procedure proved very effective and a diamide diamine was successfully synthesized.[8] Two varieties of these diamide diamines have since been synthesized (Figure 5). A butyl group was initially added to the phenyl ring to increase solubility. Further research indicated that this group was not needed and therefore a non-butyl derivative was developed.

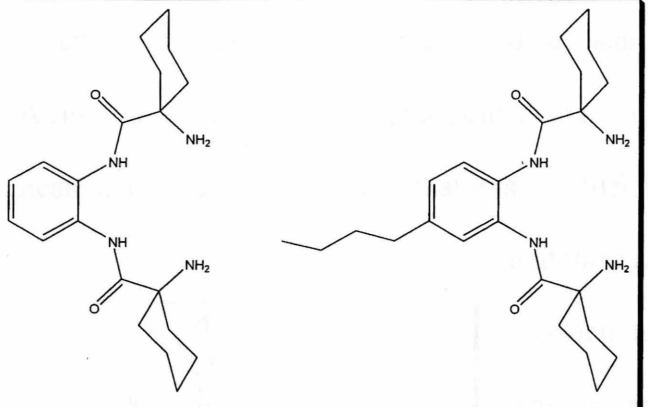

A: Non-Butyl Derivative **B**: Butyl Derivative

Figure 5: Diamide Diamine

After the successful completion of the diamide diamine, former group member Leonard Rorrer reacted both the butyl and non-butyl diamide diamines with 2,6-pyridine dicarbonyl dichloride (Figure 4B) to complete the macrocycle.[8] This reaction gave two products: the completed macrocycle and a useless polymer. To increase the yield of macrocycle, Rorrer instituted the use of high dilution conditions. This type of solvent condition proved very favorable and a 55.4 % yield was reported for the non-butyl derivative. Since the procedure for the non-butyl derivative was much more direct, less expensive and the macrocycle showed enough solubility to enable purification, all research centered on it. This new macrocycle (Figure 4C) could be produced in crystalline form in relatively high yields. The tetraamide pentadentate ligand has four metal binding amide nitrogens and one metal binding pyridine nitrogen. Despite many attempts, metalation reactions proved unsuccessful.[8]

A three pronged approach has been proposed to successfully expand the coordination chemistry of lanthanide series ions to amido-N ligands. The first is a more rigorous study of chelating the lanthanide series ion to the pentadentate macrocycle. Perhaps a more activated metal starting material will allow metalation. Early attempts into metalation proved that it is non-trivial. This does not mean that it cannot be done. Future group plans include new conditions and new starting materials.

A rigorous study of chelating the pentadentate ligand to a lanthanide series ion may indicate that it cannot be done or that it is too difficult to be done. Both the second and third approaches center on the production of new macrocyclic ligands. The first proposed ligand is a pentadentate diamide diimine macrocycle (Figure 6). The electronic structure of the pentadentate tetraamide macrocycle may be too unfavorable for metal binding. Competition from the four amide oxygens may interfere with the metal binding to the macrocyclic cavity. Imine nitrogens have been shown to bind lanthanide series ions very well.[9] The addition of imine nitrogens would give less amide oxygen competition. At this time, no steps have been taken towards the completion of this macrocycle. The pentadentate diamide diimine macrocycle is a modification of the pentadentate tetraamide macrocycle and the synthesis of it would also just be a modification of the original synthesis.

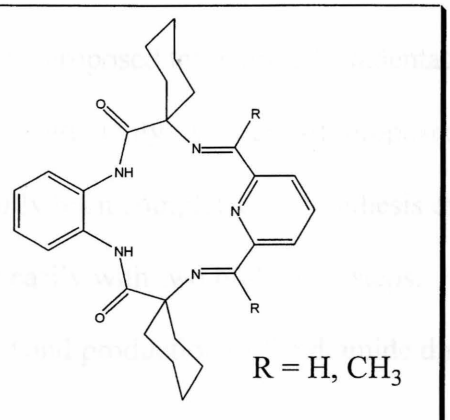

Figure 6: Pentadentate Diamide Diimine

The third approach to binding a lanthanide series ion to an amido-N ligand centers on the production of a hexadentate ligand not derived from the pentadentate ligand. It is felt the ring cavity of the pentadentate may be too small to fit a lanthanide series ion. A hexadentate ligand would potentially provide the needed increase in ring cavity size. To create this new ligand, a simple modification of the already existing pentadentate macrocycle will not suffice. An entirely new synthesis must be derived. Also, if both the electronics of the pentadentate ligand and the ring cavity size are unfavorable, a hexadentate diamide diimine ligand could be designed.

The H_4 Hexadentate Tetraamide Macrocycle

The proposed tetraamide hexadentate macrocycle (Figure 7D) has not actually been produced. Only two steps of proposed four-step synthesis (Figure 7) have successfully been completed.[10] Synthesis of the diamide dinitro (Figure 7B) intermediate proceeds easily with two high yield steps. Production of the diamide (Figure 7A) gives a 93% yield and production of the diamide dinitro gives a 91% yield. Reduction of the

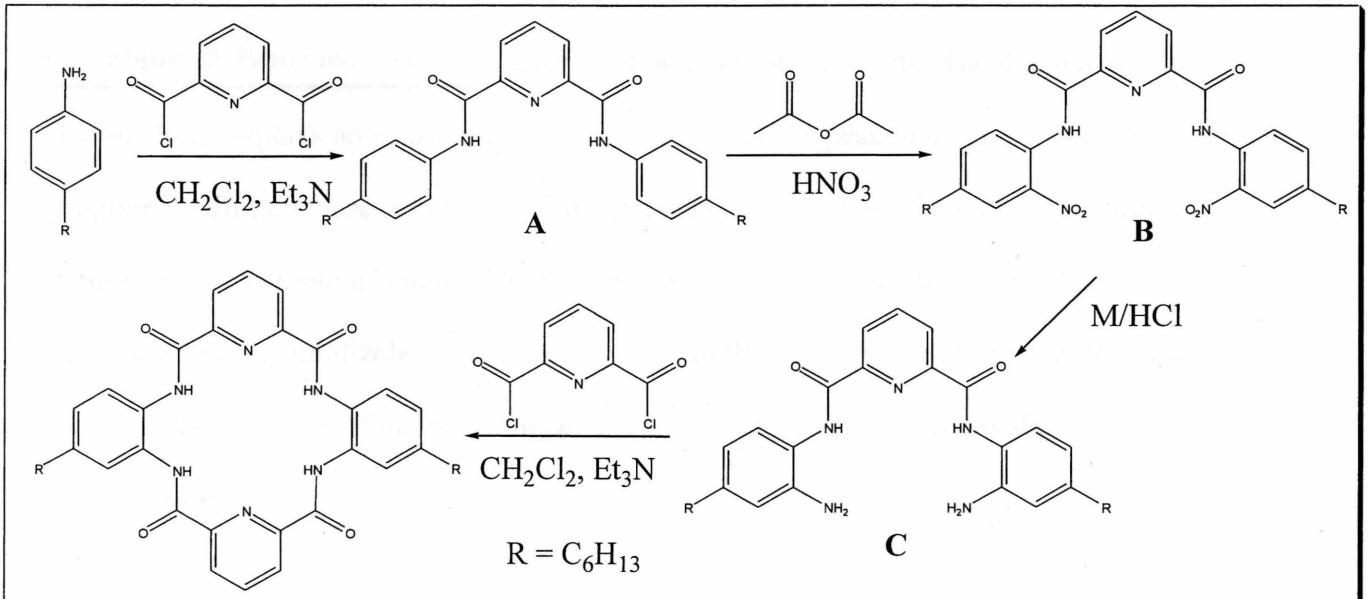

Figure 7: Synthesis of H_4 Hexadentate Macrocycle

diamide dinitro intermediate to the diamide diamine (Figure 7C) has been rather difficult.

A typical reduction involving H_2 with Pd/C could not be used because of the sensitivity of the pyridine ring. NMR data suggest that the pyridine ring is being reduced along with the nitro groups.

The next iteration of reduction attempts needed to have less harsh conditions so as to protect the pyridine ring. The most promising results came from dissolving metal reductants in an acidic medium. A solution of $TiCl_3$/HCl (8.6 wt % $TiCl_3$ in 28 wt % HCl) was reacted with the diamide dinitro intermediate. The results of this are at best inconclusive. The sensitive nature of the reaction causes small inconstancies in procedure, which lead to drastic effects in the outcome of the reaction. At this time, no one set of conditions has produced a reproducible outcome. A preliminary ^{1}H-variable temperature (VT) NMR study indicated that the proper diamide diamine will have phenyl peaks in the 6-7 ppm range. The proper product should have a doublet at 6.68 ppm, a doublet at 6.82 ppm, and a doublet of doublets at 7.22 ppm. The diamide dinitro intermediate displays no peaks in 6-7 ppm range. An NMR peak location-calculating program confirmed these results. One possible side reaction is for the reduced diamide diamine to cyclize into a benzimidizole (Figure 8). We expect that the phenyl NMR peaks for this benzimidizole would also not fall into the 6-7 ppm range. Further tests into the possible formation of the benzimidizole side product have not been conducted due to time constraints.

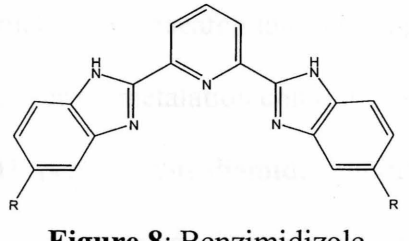

Figure 8: Benzimidizole

Other attempts with different dissolving metals have led to similar inconsistent results. A reduction with Sn metal in an acidic medium looks more promising and easier to control. Both a Fe/HCl and Zn/HCl reduction do not look as promising as either the $TiCl_3$/HCl or Sn/HCl.

After successful reduction of the nitro groups to amide groups, the completion of the macrocycle should be rather straightforward. The diamide diamine can react with 2,6-pyridine dicarbonyl dichloride to form the macrocycle. As with the pentadentate ligand, this reaction would have to run under high dilution conditions. The high dilution would again favor cyclization rather than polymer formation.

Despite many failed attempts to open the lanthanide series coordination chemistry to amido-N donors, we are confident we can find a solution to the problems. No solution at the present moment seems obvious and non-trivial. The next step may be to reestablish metalation research into the H_4 pentadentate tetraamide ligand. As presented before, differing metalation conditions may produce positive results. Also, the production of the H_2 pentadentate diamide diimine ligand should not be tremendously difficult. Perhaps the electronics of a tetraamide species is just not conducive to lanthanide series binding. The third option is to continue research into development of the H_4 hexadentate tetraamide ligand.

One solution to the reduction of the diamide dinitro to the diamide diamine problematic step is to have tighter control over the acidity of the solution. After each addition of the M/HCl mixture, the acidity of the solution spikes to a lower pH and then slowly raises as the HCl reacts. Before this reduction route is abandoned, exploration

into a low pH buffer solution is needed. The sharp drop in pH may produce the inconsistent results.

Another solution to this problem is to by-pass the reduction step. This involves a large change in the overall design of the ligand. A phenyl ring with symmetric substituents will alleviate the need for nitro groups. This level of symmetry can be achieved with the dialkoxy phenylenediamine (Figure 3) previously discussed. As explained above, research into this molecule ceased due to its extreme air sensitivity. With the new glove box, the dialkoxy phenylenediamine could be formed without ever being exposed to air. Sessler[9] et al. presents a positive synthetic route that may be feasible to the Uffelman group. The dialkoxy phenylenediamine could also be reacted with 2,6-pyridine dicarbonyl dichloride in two steps to form the macrocycle. This could possibly also proceed in one step with two equivalents of 2,6-pyridine dicarbonyl dichloride.

Experimental Section

General Experimental Information

All chemicals were ordered from Aldrich Chemicals or ACROSS and used as received. All NMR procedures were performed on a JEOL Eclipse+ 400 MHz NMR Spectrometer. All IR readings were performed on a Nicolet Impact 410 infrared spectrometer. All glove box work was performed in a Vacuum Atmosphere Nexus One inert atmosphere glove box.

Production of the H_4 Tetradentate Tetraamide Macrocycle

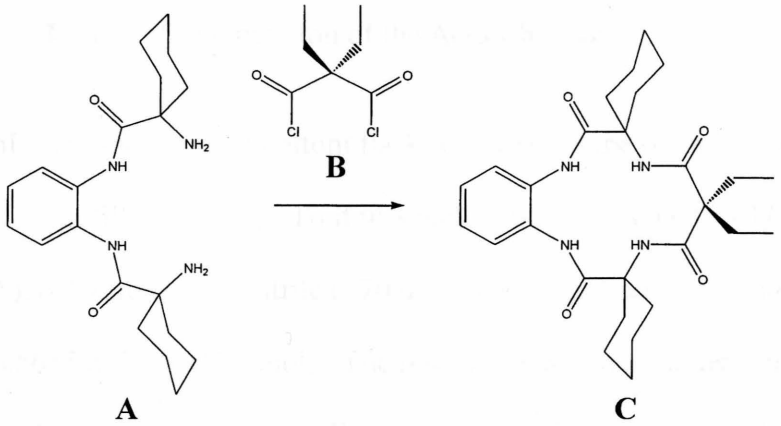

Figure 9: Preparation of H_4 Tetradentate Tetraamide Ligand

A 100 mL, three-neck, round bottom flask was connected to the Schlenk line and put under an N_2 atmosphere. It was charged with diamide diamine (0.10 g, 2.79 $x10^{-4}$ mol, Figure 9A), triethylamine, Et_3N (0.012 mL, 8.61 $x10^{-5}$ mol) and diethylmalonyl dichloride (0.005 mL, 2.91 $x10^{-5}$ mol, Figure 9B) and allowed to stir without heat (24 h). Thin-layer chromatography (TLC) in a 50/50 methylene chloride/diethyl ether solvent confirmed that there was both product and some starting material. A silica gel prep plate using the solvent diethyl ether was used to isolate the product, which was then dissolved in THF. The silica residue was filtered; the filtrate solvent was removed *in vacuo*. NMR

indicated that the known product, THF solvent, and other organic materials were present. Electrospray Mass Spectroscopy confirmed production of the product.

Production of the H_4 Pentadentate Tetraamide Macrocycle

Preparation of the Acid Chloride

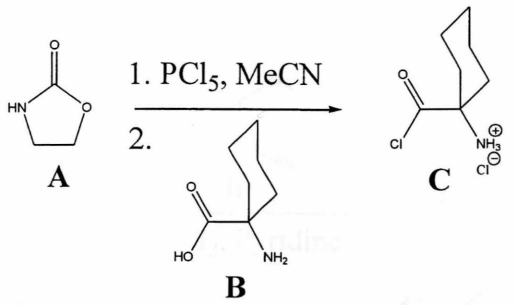

Figure 10: Preparation of the Acid Chloride

A 250 mL three-neck round bottom flask was dried in the oven, evacuated on the Schlenk line, and then filled with N_2. To it was added 2-oxazolidone (5.437 g, 6.24 x10^{-2} mol, Figure 10A), anhydrous acetonitrile (~70 mL via syringe), and phosphorus pentachloride (6.5655 g, 3.15 x10^{-2} mol). The reaction was stirred under nitrogen (24 h), and then 1-amino-1-cyclohexane carboxylic acid (2.942 g, 2.05 x10^{-2} mol, Figure 10B) was added, and the reaction was allowed to stir under nitrogen (24 h).

The reaction was stopped, filtered on a frit, and the solid was washed three times with acetonitrile (~10 mL each) and three times with methylene chloride (~10 mL each). It was dried *in vacuo* without heat. Net yield: 3.73 g, 1.88 x10^{-2} mol of Amino Acid Chloride Hydrochloride (Figure 10C) for a 91.6% yield.

Characterization: ^{1}H NMR in DMSO-d_6: δ = 1.5 (m, 10H, cyclohexane H), 6.7 (br s, 3H, amine H). ^{13}C NMR in DMSO-d_6: δ = 20.0, 25.0, 25.5, 31.0, 32.0, 63.0, 174.0. IR (Nujol): $\bar{\nu}$ (cm^{-1}) = 1735, 1768.

(This product is used as is with an approximate 9% 2-oxazolidone impurity. 2-oxazolidone spectra: ^{1}H NMR in DMSO-d_6: $\delta = 3.85$ (t), 4.3 (t). ^{13}C NMR in DMSO-d_6: $\delta = 59.0$)

Preparation of the Diamide Diamine

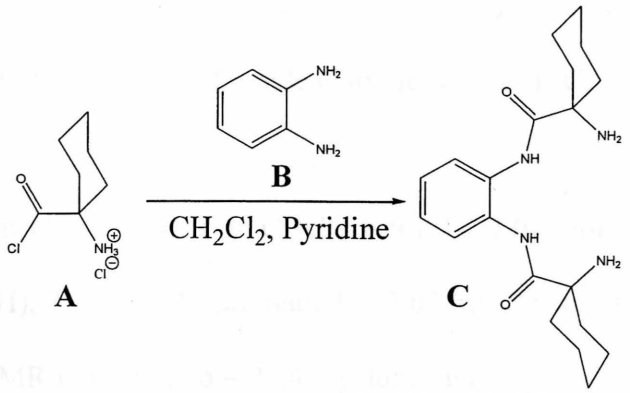

Figure 11: Preparation of the Diamide Diamine

This reaction was done via drop-wise addition to promote a higher yield. A three-neck flask was dried in the oven, placed on the Schlenk line, evacuated, and then filled with N_2. The flask was fitted with a pressure equalizing addition funnel. The flask was charged with an excess of the crude amino acid chloride hydrochloride (6.508 g, 3.29 $x10^{-2}$ mol, Figure 11A) and dry CH_2Cl_2 (~75 ml). 1,2-Phenylene diamine (1.196 g, 1.106 $x10^{-2}$ mol, Figure 11B), CH_2Cl_2 (~38 ml), and pyridine (4 ml) were added to the pressure equalizing addition funnel. The solution in the addition funnel was then added at a slow rate (2 h) to the amino acid chloride hydrochloride-CH_2Cl_2 suspension under N_2. After the addition was complete the solution with suspended solid was allowed to stir under N_2 (14 h). The solution was filtered, and the filtrate was discarded. The solid was washed with a little CH_2Cl_2, and then was dissolved in CH_2Cl_2 with the addition of aqueous NaOH. The CH_2Cl_2 solution was then extracted with aqueous NaOH three times,

keeping the organic layers. The organic layer was then dried over $MgSO_4$ and the solvent was removed under reduced pressure on a rotary evaporator. Water was added to the solid, and HCl (12 M) was added until the solid completely dissolved (pH~1). Aqueous NaOH was added to a pH~9-10. At a pH ~9-10, a white solid precipitated. The solution was filtered and the solid was washed with water. The solid was placed in a vacuum oven to dry at ~40 ^{0}C. Net yield diamide diamine (Figure 11C): 1.681 g, 4.69 x10^{-3} for a 42.3% yield.

Characterization: ^{1}H NMR in $CDCl_3$: δ = 1.3-2.2 (m, 20H, cyclohexane H), 2.15 (br s, 2H, amine H), 7.15 (m, 2H, aromatic H), 7.65 (m, 2H, aromatic H), 9.95 (s, 2H, amide H). ^{13}C NMR in $CDCl_3$: δ = 21.4 (cyclohexane C 3 or 4), 25.0 (cyclohexane C 3 or 4), 34.5 (cyclohexane C 2), 58.0 (cyclohexane C 1), 124.4 (aromatic C 3 or 4), 125.6 (aromatic C 3 or 4), 130.5 (aromatic C 1), 176.5 (carbonyl C). IR (Nujol): $\bar{\nu}$ (cm^{-1}) = 3409, 3324, 3201, 1654, 1590. Electrospray MS (positive ion mode): m/z 358.49 (M+1. 100%). Anal. Calculated for Diamide Diamine: C, 67.01; H, 8.44; N,15.63. Found: C, 66.95; H, 8.40; N, 15.56. Correlations confirmed by CH correlation spectra, Edited DEPT, and 2D COSY NMR.

Recrystallization of the diamide diamine:

A portion of the diamide diamine (0.138 g, 3.85 x10^{-4}) was dissolved in a minimal amount of CH_2Cl_2 (~5 mL). Hexanes (~5 mL) was added to the solution. The mixture was then heated to boil off the CH_2Cl_2 until the solution started to become cloudy. The solution was then removed from the heat and allowed to cool overnight during which time the diamide diamine crystallized. Net yield: 0.124 g, 3.46 x10^{-4} of recrystallized diamide diamine for a yield of 89.9%.

Preparation of the H_4 Pentadentate Tetraamide Macrocycle

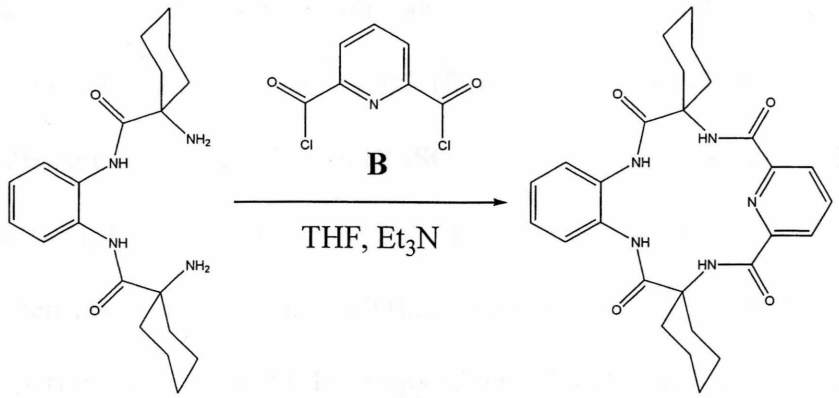

Figure 12: Preparation of H_4 Pentadentate Tetraamide Macrocycle

It was decided that in order to increase yields, high dilution conditions via syringe pumps would be used. The moisture sensitivity of the reaction dictated its performance in the glove box.

The diamide diamine (0.615 g, 1.72 $x10^{-3}$ mol, Figure 12A) was dissolved in anhydrous THF (7.5 mL) and triethylamine (0.7 mL, 5.02 $x10^{-3}$ mol). 2,6-pyridinedicarbonyl dichloride (0.352 g, 1.73 $x10^{-3}$ mol, Figure 12B) was dissolved in anhydrous THF (8.2 mL). Each solution was placed in a gas-tight syringe, and each syringe was placed on a syringe pump. The two syringes were added at 5.5 mL/hour to a common pool of THF (75 mL). The reaction was allowed to stir (24 h).

The reaction was stopped and filtered on a frit, saving the filtrate. The solvent was removed under reduced pressure on a rotary evaporator and pumped down on the Schlenk line to a solid. The solid was washed with distilled water, filtered, and pumped down on the Schlenk line. The solid was then washed with methylene chloride, filtered, and placed in a vacuum oven with minimal heat (~40 ^{o}C). Net yield (pre-crystallization): 0.465 g, 9.49 $x10^{-4}$ mol of the macrocycle (Figure 12C) for a 55.4% yield.

Characterization: ^{1}H NMR in DMSO-d_6: δ = 1.3 (s, 2H, cyclohexane H), 1.7 (s, 10H, cyclohexane H), 2.0 (d, 4H, cyclohexane H), 2.8 (m, 4H, cyclohexane H), 7.2 (m, 2H, benzene H), 7.45 (m, 2H, benzene H), 8.18 (m, 3H, pyridine H), 9.34 (s, 2H, amide H), 9.72 (s, 2H, amide H). ^{13}C NMR in DMSO-d_6: δ = 23.8 (cyclohexane C 2 or 3), 25.7 (cyclohexane C 4), 31.8 (cyclohexane C 2 or 3), 61.9 (cyclohexane C 1), 124.0 (pyridine C 4), 125.5 (benzene C 4 and C 5), 128.0 (benzene C 3 and C 6), 131.6 (benzene C 1 and C 2), 140.4 (pyridine C 3 and C 5), 149.6 (pyridine C 2 and C 6), 163.8 (carbonyl C), 171.8 (carbonyl C) IR (Nujol): $\bar{\nu}$ (cm^{-1}) = 1654, 1691, 3222, 3349, 3496. Electrospray MS (negative ion mode): m/z 489.58 (M-1. 100%). Correlations confirmed by CH correlation spectra, Edited DEPT, 2D COSY NMR, and 2D NOESY NMR.

Progress Towards the H_4 Hexadentate Tetraamide Macrocycle

Preparation of the Diamide

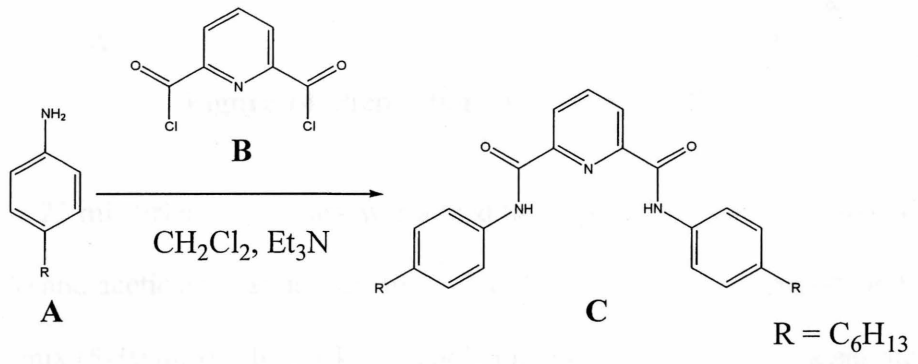

Figure 13: Preparation of the Diamide

To a 50 mL three-neck flask was added 4-hexylaniline (1 mL, 5.18 $x10^{-3}$ mol, Figure 13A), anhydrous CH_2Cl_2 (20 mL), 2,6-pyridinedicarbonyl dichloride (0.5304 g, 2.60 $x10^{-3}$ mol, Figure 13B), and Et_3N (0.723 mL). The reaction was stirred without heat under N_2 (3 h). The mixture appeared dark orange in color at the end of three hours. The

reaction was washed with aqueous Na_2CO_3 three times, keeping the organic layer. The organic layer was dried over anhydrous $MgSO_4$ and then filtered. The solvent was removed under reduced pressure and the product was dried on the Schlenk line. Net yield of diamine (Figure 13C): 1.182 g, 2.4 $x10^{-3}$ mol for 93% yield.

Characterization: ^{1}H-NMR in $CDCl_3$: δ = 0.88 (t, 6H, hexyl H's), 1.30 (m, 12H, hexyl H's), 1.63 (m, 4H, hexyl H's), 2.60 (t, 4H, hexyl H's), 7.23 (d, 4H, aromatic H's), 7.65 (d, 4H, aromatic H's), 8.13 (t, 1H, aromatic H on pyridine), 8.50 (d, 2H, aromatic H's on pyridine), 9.45 (s, 2H, amide H's). IR ($CDCl_3$): $\bar{\nu}$ (cm^{-1}) = 3388, 3154, 2925, 2859, 1816,1600, 1589, 1531.

Preparation of the Diamide Dinitro

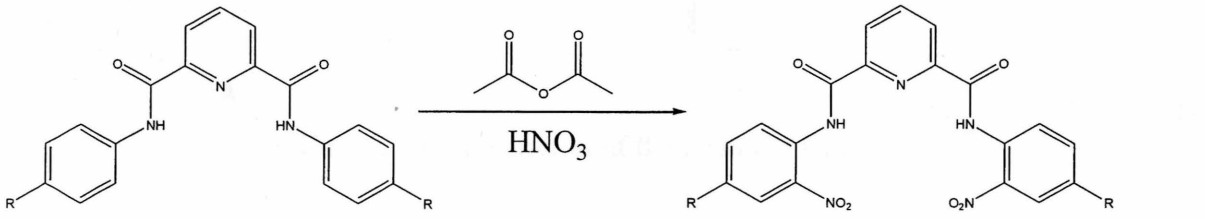

Figure 14: Preparation of the Diamide Dinitro

To a 25 mL Erlenmeyer flask was added the diamide (0.5048 g, 1.041 $x10^{-3}$ mol, Figure 14A) and acetic anhydride (3.5 mL, 3.7 $x10^{-2}$ mol). The contents of the flask were allowed to mix (5-10 min). The flask was cooled in an ice bath while concentrated HNO_3 (1.37 mL, ten fold excess) was added drop-wise. The mixture was swirled frequently. After the addition of HNO_3 was completed, the solution was stirred without heat (30 min). The reaction mixture was poured into a 50 mL beaker filled two-thirds with ice; a yellow solid precipitated and was filtered on a frit and washed with water three times.

The final product was dried *in vacuo* without heat, since the product melts with low heat. Net Yield of Diamide Dinitro (Figure 14B): 0.541 g, 9.4 x10^{-4} mol for 90.5% yield.

Characterization: ^{1}H-NMR in $CDCl_3$: δ = 0.89 (t, 6H, hexyl H's), 1.32 (m, 12H, hexyl H's), 1.65 (m, 4H, hexyl H's), 2.68 (t, 4H, hexyl H's), 7.55 (dd, 2H, aromatic H's), 8.08 (d, 2H, aromatic H's), 8.18 (t, 1H, aromatic H's), 8.50 (d, 2H, aromatic H's), 8.77 (d, 2H, aromatic H's), 12.36 (s, 2H, amide H's). IR ($CDCl_3$) = 3309, 3154, 2931, 2857, 1816, 1697, 1519,1463.

Preparation of the Diamide Diamine

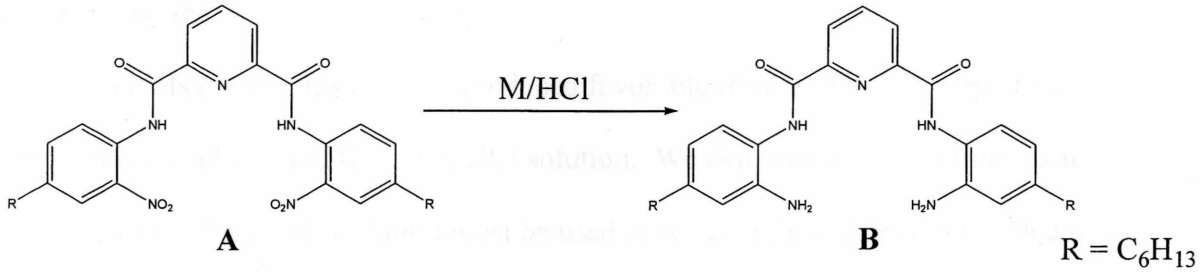

Figure 15: Preparation of the Diamide Diamine

As previously stated, no one set of reaction conditions produced a repeatable product. This reaction is not fully understood at this time. Here, the procedures with the best results are presented. The reactions presented here of $TiCl_3$/HCl and Sn/HCl we believe produced the correct diamide diamine (Figure 15B). The characterization shown is from these presumably correct reactions.

Characterization: ^{1}H NMR in DMSO-d_6: δ = 0.88 (t, 9H, hexyl H's), 1.30 (m, 20H, hexyl H's), 1.56 (m, 7H, hexyl H's), 1.78 (m, 2H, hexyl H's), 2.1 (s, 2H, hexyl H's), 3.44 (t, 2H, hexyl H's), 3.64 (t, 2H, hexyl H's), 6.68 (d, 2H, aromatic H's), 6.82 (d, 2H, aromatic H's), 7.22 (dd, 2H, aromatic H's), 8.27 (m, 1H, aromatic H's), 8.34 (s, 1H, aromatic H's), 8.36 (d, 1H, aromatic H's).

The $TiCl_3$/HCl Reaction

To a 25 mL three-neck flask diamide dinitro (0.05 g, 8.7 x10^{-5} mol, Figure 16A) and THF (10 mL) were added under N_2. Then $TiCl_3$ (0.54 mL, 8.6 wt % $TiCl_3$ in 28 wt % HCl) was added to the solution via syringe. The mixture was allowed to stir (1-2 h) under N_2. A second aliquot of $TiCl_3$ (1 mL, 7.7 x10^{-3} mol) was added. The mixture was again allowed to stir (1-2 h) under N_2. The reaction mixture was then made basic with aqueous Na_2CO_3. To the basic solution was added CH_2Cl_2, and the organic layer was separated and the organic solvent was then removed under reduced pressure and dried on the Schlenk line.

Initials runs of this reaction produced favorable results. The key step of the reaction is the addition of the $TiCl_3$/HCl solution. We determined that a multi aliquot addition of the $TiCl_3$/HCl solution must be used to produce favorable results. One large injection tended to yield a mess of products. Perhaps having too much metal reactant in solution produced these unfavorable results, or maybe the pH became too low.

The Sn/HCl Reaction

A 50 mL three-neck flask was dried and placed under an N_2 atmosphere. The diamide dinitro (0.105 g, 1.74 x10^{-4} mol, Figure 16A) was added to the flask along with THF (25 mL). This mixture was let stir (1-2 min) before adding the Sn (0.497 g, 4.19 E^{-3} mol, 24 equivalents) and HCl (0.347 mL, 12 M, 24 equivalents). After allowing the reaction to stir (overnight, approx. 18 h), Na_2CO_3 was added until a basic pH was achieved. The reaction mixture was extracted three times with CH_2Cl_2, saving the organic layer. The organic layer was dried over $MgSO_4$ before removing the solvent *in vacuo*.

When performed on this small scale, the purification process seemed to work well. Any attempt to increase the scale produced very odd and unique results, especially in the extraction step. Many reactions gave a terrible emulsion that could not be separated by adding acetone or NaCl. Reactions that did not produce the emulsion tended to separate into two layers, with the aqueous layer being more dense (i.e. as the bottom layer) than the organic layer. At this point we have no explanation as to how or why this occurred. Upon basification with Na_2CO_3, a white slushy "solid" substance would appear in some reactions. Attempting to filter this solid with a frit became very messy; the solid clogged every frit used. No data of the substance could ever be recorded thus it is not known what the substance is. It is felt that this substance needs to filtered away from the reaction mixture before the extraction step. Conceivably, this solid causes the emulsion. Much work is needed on both the reaction conditions and the purification steps.

The Fe/HCl Reaction

To a 100 mL three-neck flask, dried and put under an N_2 atmosphere, was added the diamide dinitro (0.104 g, 1.81 $x10^{-4}$ mol, Figure 16A). After addition of THF (25 mL) the reaction was allowed to stir (1-2 min). Then HCl (0.343 mL, 12 M, 24 equivalents) was added along with Fe metal (0.233 g, 24 equivalents). The reaction was allowed to stir (overnight, approx. 12 hours). TLC indicated no product formation. This reaction was not worked up. Only a few attempts of this reaction were performed. More research into this reaction should be conducted in the future.

The Zn/HCl Reaction

A 100 mL three-neck flask was dried and placed under a N_2 atmosphere. To the flask was added the diamide dinitro (0.100 g, 1.74 $x10^{-4}$ mol, Figure 16A) with THF (25 mL). After allowing the reaction to stir (1-2 min), HCl (0.343 mL, 12 M, 24 equivalents) was added along with Zn metal (0.273 g, 24 equivalents). The reaction was allowed to stir (overnight, approx. 12 hours) before taking a TLC. The TLC indicated no product formation. This reaction was performed at the end of the term and not much time was devoted to it. More research should be put towards this reaction.

While some of these reduction reactions seemed promising and others seemed not, all should be attempted again in the future. Because we have little understanding of why we obtained these results, slight changes in conditions and purification may produce favorable results.

References

[1] Comblin, V.; Gilsoul, D.; Hermann, M.; Humblet, V.; Jacques, V.; Mesbahi, M.; Sauvage, C.; Desreux, J. F. "Designing new MRI Contrast Agents: A Coordination Chemistry Challenge." *Coord. Chem. Rev.* **1999**, *185-186*, 451-470.

[2] Sessler, J. L.; Mody, T. D.; Hemmi, G. W.; Lynch, V.; Young, S. W.; Miller, R. A. "Gadolinium(III) Texaphyrin: A Novel MRI Contrast Agent." *J. Am. Chem. Soc.* **1993**, *115*, 10368-10369.

[3] Amie, S.; Botta, M.; Crich, S. G.; Giovenzana, G. B.; Jommi, G.; Pagliarin, R.; Sisti, M. "MRI Contrast Agents: Macrocyclic Lanthanide(III) Complexes with Improved Relaxation Efficiency." *J. Chem. Soc., Chem. Commun.* **1995**, 1885-1886.

[4] Collins, T. J.; Kostka, K. L.; Uffelman, E. S.; Weinberger, T. L. "Design, Synthesis, and Structure of a Macrocyclic Tetraamide That Stabilizes High-Valent Middle and Later Transition Metals." *Inorg. Chem.* **1991**, *30*, 4204-4210.

[5] Uffelman, E. S. Ph.D. Dissertation, California Institute of Technology, Pasadena, CA, 1991.

[6] Rorrer, L. C.; Hopkins, S. D.; Connors, M. K.; Lee III, D. W.; Smith, M. V.; Rhodes, H. J.; Uffelman, E. S. "A Convenient New Route to Tetradentate and Pentadentate Macrocyclic Tetraamide Ligands" *Org. Lett.* **1999**, *1*, 1157-1159.

[7] Polomo Coll, A. L.; Meseguer, J. D. U.S. Patent 4,230,849. 1985.

[8] Rorrer, L. C.; Hopkins, S. D.; Connors, M. K. Final Report. R.E. Lee Fellowship, Washington and Lee University, Lexington, VA, 1998.

[9] Sessler, J. L.; Mody, T. D.; Hemmi, G. W.; Lynch, V. "Synthesis and Structural Characterization of Lanthanide(III) Texaphyrins." *Inorg. Chem.* **1993**, *32*, 3175-3187.

[10] Hopkins, S. D.; Shreves, A. E.; Cartwright, A. R.; Stoklasek, T. A. Final Report. R.E. Lee Fellowship, Washington and Lee University, Lexington, VA, 1999.

ORGANIC LETTERS

1999
Vol. 1, No. 8
1157–1159

A Convenient New Route to Tetradentate and Pentadentate Macrocyclic Tetraamide Ligands

Leonard C. Rorrer, Stephen D. Hopkins, Michele K. Connors, Daniel W. Lee III, Matthew V. Smith, Hilary J. Rhodes, and Erich S. Uffelman*

Department of Chemistry, Washington and Lee University, Lexington, Virginia 24450

uffelman.e@wlu.edu

Received July 9, 1999

ABSTRACT

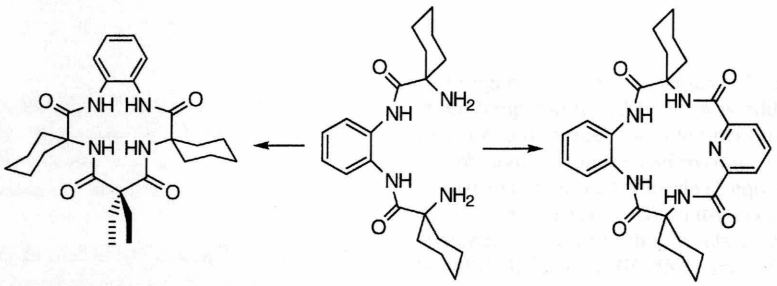

A crucial diamide diamine intermediate in the synthesis of tetradentate macrocyclic tetraamide ligands protected against oxidative decomposition has been synthesized without the use of potentially hazardous organic azide intermediates. This intermediate has also been used to synthesize a new class of pentadentate macrocyclic tetraamide ligands.

Since the potential importance to inorganic chemistry of macrocyclic tetraamide ligands protected against oxidative decomposition was first demonstrated,[1] these ligands have been used to synthesize a variety of rare or unprecedented oxidation states, geometries, and spin states of chromium, manganese, iron, cobalt, nickel, and copper.[1,2] When a two-step route to these macrocycles that did not involve organic azides was developed,[3] transition metal complexes of these ligands suddenly had the potential to become valuable homogeneous catalysts.[4] Recent work has demonstrated the utility of these catalysts in the important emerging field of green chemistry (bleaching and pulp and paper applications).[5]

We have been working to produce expanded macrocyclic tetraamide ligands for possible use with lanthanides and for multimetallic applications. In the process of solving difficulties we encountered in synthesizing a new class of tractable pentadentate macrocyclic tetraamide ligands, we have gener-

(1) (a) Collins, T. J.; Uffelman, E. S. *Angew. Chem., Int. Ed. Engl.* **1989**, *28*, 1509–1511. (b) Uffelman, E. S. Ph.D. Dissertation, California Institute of Technology, Pasadena, CA, 1991.

(2) (a) Collins, T. J.; Powell, R. D.; Slebodnick, C.; Uffelman, E. S. *J. Am. Chem. Soc.* **1990**, *112*, 899–901. (b) Collins, T. J.; Kostka, K. L.; Münck, E.; Uffelman, E. S. *J. Am. Chem. Soc.* **1990**, *112*, 5637–5639. (c) Collins, T. J.; Nichols, T. R.; Uffelman, E. S. *J. Am. Chem. Soc.* **1991**, *113*, 4708–4709. (d) Collins, T. J.; Slebodnick, C.; Uffelman, E. S. *Inorg. Chem.* **1990**, *29*, 3432–3436. (e) Collins, T. J.; Kostka, K. L.; Uffelman, E. S.; Weinberger, T. *Inorg. Chem.* **1991**, *30*, 4204–4210. (f) Collins, T. J.; Powell, R. D.; Slebodnick, C.; Uffelman, E. S. *J. Am. Chem. Soc.* **1991**, *113*, 8419–8425. (g) Collins, T. J. *Acc. Chem. Res.* **1994**, *27*, 279–285.

(3) (a) Gordon-Wylie, S. W. Ph.D. Dissertation, Carnegie Mellon University, Pittsburgh, PA, 1995. (b) Gordon-Wylie, S. W.; Collins, T. J. U.S. Patent Allowed.

(4) (a) Bartos, M. J.; Gordon-Wylie, S. W.; Fow, B. G.; Wright, L. J.; Weintraub, S. T.; Kauffmann, K. E.; Münck, E.; Kostka, K. L.; Uffelman, E. S.; Rickard, C. E. F.; Noon, K. R.; Collins, T. J. *Coord. Chem. Rev.* **1998**, *174*, 361–390. (b) Miller, C. G.; Gordon-Wylie, S. W.; Horwitz, C. P.; Strazisar, S. A.; Peraino, D. K.; Clark, G. R.; Weintraub, S. T.; Collins, T. J. *J. Am. Chem. Soc.* **1998**, *120*, 11540–11541. (c) Horwitz, C. P.; Fooksman, D. R.; Vuocolo, L. D.; Gordon-Wylie, S. W.; Cox, N. J.; Collins, T. J. *J. Am. Chem. Soc.* **1998**, *120*, 4867–4868. (d) Patterson, R. E.; Gordon-Wylie, S. W.; Woomer, C. G.; Norman, R. E.; Weintraub, S. T.; Horwitz, C. P.; Collins, T. J. *Inorg. Chem.* **1998**, *37*, 4748–4750.

(5) Collins, T. J.; Gordon-Wylie, S. W.; Bartos, M. J.; Horwitz, C. P.; Woomer, C. G.; Williams, S. A.; Patterson, R. E.; Vuocolo, L. D.; Paterno, S. A.; Strazisar, S. A.; Peraino, D. K.; Dudash, C. A. In *Green Chemistry: Frontiers in Benign Chemical Syntheses and Processes*; Anastas, P. T., Williamson, T. C., Eds.; Oxford University Press: Oxford, U.K., 1998; pp 46–71.

10.1021/ol990155f CCC: $18.00
Published on Web 09/23/1999

ated a valuable, convenient new method for synthesizing tetradentate macrocyclic tetraamide ligands.

Our synthesis of **5** (R = Me) proceeded by an organic azide route to the diamide diamine intermediate **4** (Scheme 1). This route to **4** was known from prior work.[1b,2f]

Scheme 1. Synthesis of an Intractable Macrocycle via an Old Azide Route[a]

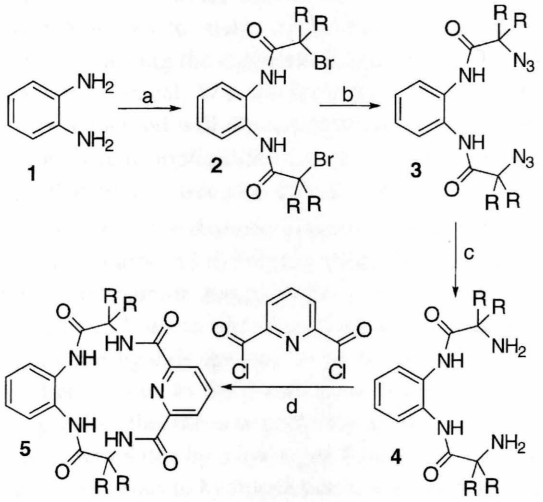

[a] Legend: (a–c) 2-bromoisobutyryl bromide, then NaN_3, then H_2, Pd/C (see refs 1b and 2f); (d) product quite insoluble, yield undetermined, product identified by FAB MS.

Unfortunately, **5** (R = Me) is sparingly soluble in DMSO and DMF and is insoluble in other common lower boiling organic solvents. Conceptually, greater organic solubility could be designed into the molecule in three places: by varying the aromatic ring substituents, by varying the R groups, or by varying the substituents on the pyridine ring. Increasing the size of the R groups destroys the viability of the azide route. Efforts to synthesize **5** (R = Pr) via the azide route were thwarted by considerable elimination.

In the redesign of the synthesis, we recognized that it is desirable to employ highly reactive acylating agents with 1,2-phenylenediamines, since the production of benzimidazoles can be a competing side reaction even with acid chlorides.[6] Indeed, 1,2-phenylenediamines that are even weakly deactivated by other substituents on the benzene ring often yield benzimidazoles exclusively when acylation is attempted with reagents less active than acid chlorides.[6] This factor renders much of the protected amino acid coupling technology developed for biochemistry inapplicable to macrocyclic systems such as **5**, **9**, and **10**. Clearly, **5**, **9**, and **10** are conceptually composed of 1,2-phenylenediamine, 2 equiv of an amino acid, and either 2,6-pyridinedicarboxylic acid or diethylmalonic acid.

Our new method of synthesizing these crucial diamide diamine intermediates, **4** and **8**, is derived from the antibiotic synthesis patent literature,[7] and it allows us to generate a very reactive acylating agent (the acid chloride), using the proton as a protecting group. As an example (Scheme 2),

Scheme 2. Synthesis of a Key Diamide Diamine Intermediate and Its Conversion to Tractable Macrocycles[a]

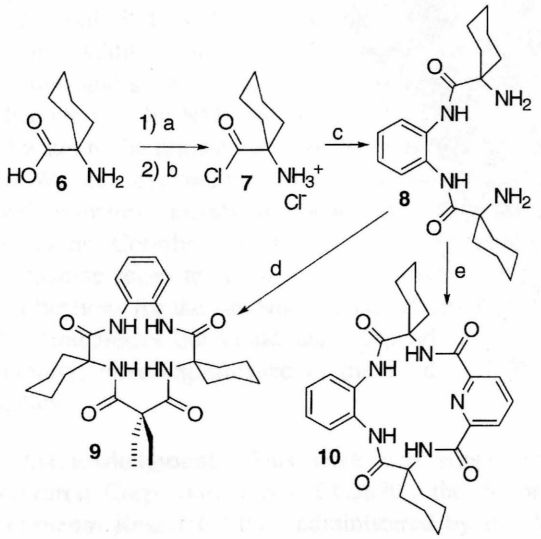

[a] Legend: (a) PCl_5 (1 equiv), 2-oxazolidone (2 equiv), MeCN, room temperature, 12 h; (b) **6** is added to the PCl_5/2-oxazolidone mixture and stirred, room temperature, 12 h, 92%; (c) solution of 1,2-phenylenediamine and pyridine (2.2 equiv) slowly added (2 h) to suspension of acid chloride (2 equiv), CH_2Cl_2, room temperature, 12 h, 42%, see ref 8; (d) diethylmalonyl dichloride, CH_2Cl_2, 25% (procedure similar to that in refs 1b and 2f); (e) 2,6-pyridinedicarbonyl dichloride, THF, 55%, see refs 9 and 13.

PCl_5 was stirred with 2-oxazolidone, followed by the addition of 1-amino-1-cyclohexanecarboxylic acid (**6**). The resulting salt, **7**, is easily isolated by filtration and is used as is, even though it is slightly contaminated with 2-oxazolidone. Slow addition of 1,2-phenylenediamine yields the diamide diamine product **8**.[8] Addition of diethylmalonyl dichloride gives **9** in 25% yield (the NMR, electrospray MS, and IR data for this compound are identical with the data for the same compound produced by the patented method[3,4d]).

It should be noted that this synthetic method holds great promise for introducing chirality into the macrocyclic tetraamide ligands via α-disubstituted amino acids bearing different R groups. Furthermore, recent research has revealed that although the metalated macrocyclic tetraamide ligands are extraordinarily robust under oxidizing conditions, high-valent iron-oxo species formed from these macrocycles

(6) Keech, J. T. Ph.D. Dissertation, California Institute of Technology, Pasadena, CA, 1986.

(7) Palomo Coll, A. L.; Meseguer, J. D. U.S. Patent 4 230 849, 1985.

(8) Characterization of **8**: ^1H NMR (in $CDCl_3$) δ 1.3–2.2 (m, 20H, cyclohexane H), 2.15 (br s, 4H, amine H), 7.15 (m, 2H, aromatic H), 7.65 (m, 2H, aromatic H), 9.95 (s, 2H, amide H); ^{13}C NMR (in $CDCl_3$) δ 21.4 (cyclohexane C-3 or C-4), 25.0 (cyclohexane C-3 or C-4), 34.5 (cyclohexane C-2), 58.0 (cyclohexane C-1), 124.4 (aromatic C-3 or C-4), 125.6 (aromatic C-3 or C-4), 130.5 (aromatic C-1), 176.5 (carbonyl C); NMR assignments confirmed by CH correlation spectra, edited DEPT, and 2D COSY NMR; IR (Nujol) $\bar{\nu}$ (cm^{-1}) 3409, 3324, 3201, 1654, 1590; electrospray MS (positive ion mode) *m/z* 358.49 (M + 1, 100%). Anal. Calcd for diamide diamine: C, 67.01; H, 8.44; N, 15.63. Found: C, 66.95; H, 8.40; N, 15.56.

ultimately decompose slowly via intramolecular hydrogen atom abstraction from the methylene carbon of the diethylmalonamide unit.[4a] Substitution chemistry at this site has already generated even more robust catalyst systems.[4c] The prior non-azide route involves coupling 2 equiv of amino acid with diethylmalonyl dichloride to generate a diamide dicarboxylic acid, which is then coupled with a 1,2-phenylenediamine derivative to yield product.[3] Large amounts of pyridine solvent are used in both steps. Our new synthetic route promises to make the systematic exploration of the effect of varying the malonamide groups more efficient and more economical. We anticipate that the prior method and our new method will ultimately be complementary in terms of commercial applicability; i.e., each method appears to have complementary strengths and limitations.

Reaction of the diamide diamine intermediate **8** with 2,6-pyridinedicarbonyl dichloride yields a new class of pentadentate tetraamide macrocycles in a remarkable 55% yield (Scheme 2).[9] Just as one class of the tetradentate macrocyclic tetraamide ligands appears to be templated by a hydrogen bond analogous to the β-turn seen in protein folding,[1b,2e,10] it is possible that the new pentadentate tetraamide macrocycle may be templated by a hydrogen bond involving the pyridine that is analogous to hydrogen bonds seen with amides derived from 2,6-pyridinedicarboxylic acid for catenanes[11] and helical supramolecular arrays.[12] This new pentadentate tetraamide macrocycle, **10**, has been characterized by ^{1}H NMR, ^{13}C NMR, C−H correlation spectra, edited DEPT, 2D COSY, 2D NOESY, IR, and electrospray MS.[13] The new pentadentate macrocycles show cross-peaks in the 2D NOESY spectra for the amide protons, indicating that they are in close proximity to each other. Not only is the geometric proximity of the amide protons consistent with a hydrogen bond template in the final coupling reaction, the pentadentate tetraamide macrocycles do not exhibit a change in the ^{1}H NMR in the presence of strong acids, indicating that the pyridine ring is extraordinarily difficult to protonate.

Not only is **10** stable in concentrated acid, it is also base-stable. Addition of 4 equiv of LDA removes the amide protons and generates a lithiated tetraanion which we have characterized by NMR in THF-d_8 and DMSO-d_6. Addition of water to the lithiated tetraanion quantitatively regenerates **10**. We are surveying the reactivity of the lithiated tetraanion with transition metals and with the lanthanide series of trications. Coordinating the organic amido-*N* ligand to a lanthanide series trication would not only have significant implications for the fundamental coordination chemistry of the lanthanides but could also, depending on hydrolytic stability, have significance to the field of MRI contrast agents.

Acknowledgment. This work was supported by the Research Corp. (Grant No. CC3870), the donors of the Petroleum Research Fund, administered by the American Chemical Society (Grant No. 29495-GB3), and the National Science Foundation (Grant No. DUE−9650033). This work was also supported by Washington and Lee Summer Research Student Fellowships, Glenn Grants, and a Class of '65 Excellence in Teaching Award. We thank Mr. Sayam Sen Gupta of Carnegie Mellon University for the electrospray MS data. We are indebted to Dr. Terrence J. Collins (Carnegie Mellon University) and Dr. Scott Gordon-Wylie (University of Vermont) for useful discussions and preprints of publications. This work is dedicated to Dr. Collins in recognition of his recent Presidential Green Chemistry Challenge Award and to Dr. Charles A. Root on the occasion of his retirement from Bucknell University.

OL990155F

(9) Synthesis of **10**: compound **8** (0.615 g, 0.00172 mol) was dissolved in anhydrous THF (7.5 mL) and triethylamine (0.7 mL, 0.00502 mol). 2,6-Pyridinedicarbonyl dichloride (0.352 g, 0.00173 mol) was dissolved in anhydrous THF (8.2 mL). Each solution was added to a common pool of THF (75 mL) via syringe pump (1.5 h). The reaction mixture was stirred (24 h) and then filtered, saving the filtrate. The filtrate was taken to dryness under reduced pressure. The resultant solid was washed with distilled water, filtered, and pumped to dryness. The solid was then washed with methylene chloride, filtered, and dried under vacuum oven (~40 °C). Net yield: 0.465 g, 0.000 949 mol, 55.4%. The macrocycle is recrystallized in high yield by vapor diffusion of hexanes into a THF solution.

(10) (a) Dado, G. P., Desper, J. M.; Gellman, S. H. *J. Am. Chem. Soc.* **1990**, *112*, 8630−8632. (b) Gellman, S. H.; Dado, G. P.; Liang, G.-P.; Adams, B. R. *J. Am. Chem. Soc.* **1991**, *113*, 1164−1173.

(11) (a) Hunter, C. A.; Purvis, D. H. *Angew Chem., Int. Ed. Engl.* **1992**, *31*, 792−794. (b) Hunter, C. A. *J. Am. Chem. Soc.* **1992**, *114*, 5303−5311. (c) Carver, F. J.; Hunter, C. A.; Shannon, R. J. *J. Chem. Soc., Chem. Commun.* **1994**, 1277−1279.

(12) (a) Kawamoto, T.; Prakash, O.; Ostrander, R.; Rheingold, A. L.; Borovik, A. S. *Inorg. Chem.* **1995**, *34*, 4294−4295. (b) Kawamoto, T.; Hammes, B. S.; Haggerty, B.; Yap, G. P. A.; Rheingold, A. L.; Borovik, A. S. *J. Am. Chem. Soc.* **1996**, *118*, 285−286.

(13) Characterization of **10**: ^{1}H NMR (in DMSO-d_6) δ 1.3 (s, 2H, cyclohexane H), 1.7 (s, 10H, cyclohexane H), 2.0 (d, 4H, cyclohexane H), 2.8 (m, 4H, cyclohexane H), 7.2 (m, 2H, benzene H), 7.45 (m, 2H, benzene H), 8.18 (m, 3H, pyridine H), 9.34 (s, 2H, amide H), 9.72 (s, 2H, amide H); ^{13}C NMR in (DMSO-d_6) δ 23.8 (cyclohexane C-2 or -3), 25.7 (cyclohexane C-4), 31.8 (cyclohexane C-2 or -3), 61.9 (cyclohexane C-1), 124.0 (pyridine C-4), 125.5 (benzene C-4 and C-5), 128.0 (benzene C-3 and C-6), 131.6 (benzene C-1 and C-2), 140.4 (pyridine C-3 and C-5), 149.6 (pyridine C-2 and C-6), 163.8 (carbonyl C), 171.8 (carbonyl C); NMR assignments confirmed by CH correlation spectra, edited DEPT, 2D COSY NMR, and 2D NOESY NMR; IR (Nujol) $\bar{\nu}$ (cm^{-1}) 3496, 3349, 3222, 1691, 1654; electrospray MS (negative ion mode) *m/z* 489.58 (M − 1, 100%).